Effects of Input Frequency and Reticular Inhibition on a Firing-Rate Model of Retinogeniculate Transmission

A thesis submitted in partial fulfillment of the requirement
for the degree of Bachelor of Science in Physics
from the College of William and Mary in Virginia,

by

Paul Eugene Brewer

Adviser: Dr. Gregory D. Smith

Williamsburg, Virginia
May 2003

Abstract

The thalamus is a major hub of communication in the mammalian brain. It relays all sensory input (except olfactory) from the sensory organs to the cortex and also oversees the transfer of information between areas of the cortex. However, it is unknown how the thalamus modifies the information it transfers. The dorsal lateral geniculate nucleus (dLGN), a visually-responsive nucleus of the thalamus, receives information from the retina and projects it on to primary visual cortex. Relay neurons of the dLGN (thalamocortical neurons) are connected in a feedback loop to inhibitory neurons of the perigeniculate nucleus (reticular neurons). Here we investigate the possible consequences of this feedback loop using a mathematical model of thalamocortical and reticular neuron firing rates. We quantify the influence of reticular inhibition and retinal stimulus envelope frequency on the transmission properties of a thalamocortical-reticular neuron pair. We find that reticular inhibition frequently causes high-pass filtering and phase-advancing of the transferred signal.

Acknowledgements

I am greatly indebted to Dr. Smith for his generous patience, time and support. Early investigation for this research was supported by the College of William and Mary physics REU program.

Contents

1 Introduction

1.1 The Thalamus

The mammalian thalamus is a small region of the brain located below the corpus callosum (see Fig. 1). The nervous tissue that carries sensory information from each sensory organ to the higher brain is called the sense's 'pathway'. The thalamus is at the center of all sensory organ pathways, except olfactory. Accordingly, it relays information from the sensory organs to the proper cortical areas. It also performs intracortical information transfer, relaying signals from one cortical area to another.

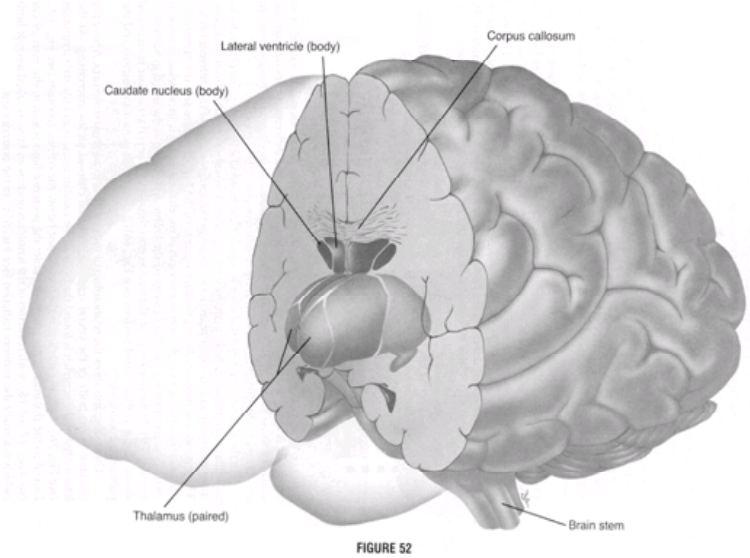

Figure 1: Human brain with thalamus [3].

One of the sensory pathways is the primary visual pathway. In mammals, this pathway extends from the retinal ganglion cells (RGC) to the primary visual cortex (V1), passing through the dorsal lateral geniculate nucleus (dLGN) of the thalamus. Within the dLGN, thalamocortical (TC) neurons receive the retinal signals and relay this information on to V1. This process is called retinogeniculate transmission. The TC neurons also receive input from other sources including local interneurons, subcortical areas, striate cortex and reticular

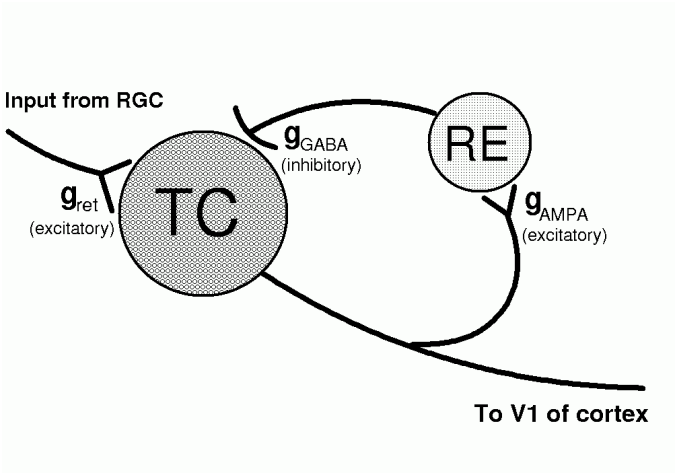

Figure 2: A diagram of the TC-RE feedback loop.

(RE) neurons of the perigeniculate nucleus (PGN) [1]. Of all these non-retinal inputs, the inhibitory input from RE is one of the strongest [9]. In addition, the RE neurons receive an excitatory input (an axon-collateral) associated with the TC→cortex projection (see Fig. 2). Thus, the TC neurons are in a negative feedback loop with the RE neurons. Even though the RE inhibiton appears to have an influential role in retinogeniculate transmission, the effect has never been quantified [8]. The focus of this research was to determine the effect of RE cell inhibition on the transmission properties of the TC-RE network, where RGC cell activity is considered as the 'input', and TC cell activity the output.

1.2 Neural Behavior

An action potential is the only fluctuation in neural membrane potential that can propagate over large distances [1]. Because subthreshold fluctuations dissipate over short distances ($\leq$ 1mm) [1], the primary vehicle for information transfer between neurons is the action potential. An action potential is a rapid depolarization of a neural membrane that, in many cases, originates in the cell soma and propagates down the axon to synapses. Once this wave of depolarization reaches the synapses, the voltage change causes axonal vesicles of the presynaptic cell to fuse with the cell membrane and release small signalling molecules known as neurotransmitters. These neurotransmitters then bind to receptors located on the den-

drites of the postsynaptic neuron. When a neurotransmitter binds to a receptor, ion channels in the post-synaptic neuron's membrane change state thus affecting the flux of certain ions through the membrane. 'Excitatory' neurotransmitters cause the post-synaptic neuron's membrane to depolarize, sometimes generating an action potential. Conversely, 'inhibitory' neurotransmitters cause the post-synaptic cell to hyperpolarize, making the production of an action potential less likely. 'Excitatory' and 'inhibitory' neurons can be identified by the type of neurotransmitter secreted and their influence on down-stream neurons.

For certain types of sensory neurons, the specific timing of action potentials has been demonstrated to be functionally important [9]. However, for many neurons it is the change in the time-averaged firing frequency of incoming action potentials, not the precise spike times of every action potential, that is of primary physiological significance. There is no evidence to date that indicates that precise spike timing is functionally important to retinogeniculate transmission.

1.3 Mathematical Models of Neural Responses

Hodgkin-Huxley Model

The Hodgkin-Huxley (HH) model of the squid giant axon was the first succesful mathematical model of the membrane excitability responsible for action potential propagation. Created by Hodgkin and Huxley in the 1950's, this model simulates the dynamics of a cell's membrane potential by numerically integrating four differential equations [4]. Three ODEs determine the dynamics of gating variables for two membrane conductances (Eqs. 2-4). The fourth equation represents the balance of applied, membrane, and capacitive currents (Eq. 1). The Hodgkin-Huxley equations are:

$$C\frac{dV}{dt} = I_{app} - g_{Na_0}m^3h(V - V_{Na}) - g_{K_0}n^4(V - V_K) - g_L(V - V_L) \quad (1)$$

$$\frac{dn}{dt} = \alpha_n(V)(1 - n) - \beta_n(V)n \quad (2)$$

$$\frac{dm}{dt} = \alpha_m(V)(1 - m) - \beta_m(V)m \quad (3)$$

$$\frac{dh}{dt} = \alpha_h(V)(1-h) - \beta_h(V)h \tag{4}$$

where, C is the membrane capacitance, V is the membrane potential, I_{app} is an applied current, g_{Na_0} is the conductance of the sodium ion current, g_{K_0} is the conductance of the potassium ion current, g_L is the conductance of the leakage current (leaking to extracellular regions), V_{Na}, V_K and V_L are the reversal potentials of their respective currents, and m, n, and h are gating variables of the ion currents. The speed and voltage at which the ion currents open and close are determined by the α and β variables.

Although the equations and parameters of the HH model were chosen to represent membrane excitability of the squid giant axon, HH-style modeling of neuronal membranes has become a traditional approach in computational neuroscience [9].

Integrate-and-Fire Models

Integrate-and-Fire (IF) models are similar to HH style models in that they involve a current balance equation. However, rather than expicitly modeling action potential-generating currents, the event times of instantaneous spikes are determined by the membrane potential reaching a specified threshold value, V_θ. When spikes occur, the membrane potential is reset to a specified voltage, V_{reset}. After an absolute refractory period the membrane potential can integrate subsequent input and eventually spike again [6].

The integrate-and-fire equations are

$$C\frac{dV}{dt} = I_{app} - g_{leak}(V - V_{leak}) \tag{5}$$
$$V(t^-) = V_\theta \rightarrow V(t^+) = V_{reset} \ .$$

Notice that if there were no threshold for spiking the steady-state voltage, V_{SS}, would be given by:

$$V_{SS} = V_{leak} + I_{app}/g_{leak} \ .$$

Setting $V_{SS} > V_\theta$ we see that the IF model neuron spikes repetitively when

$$I_{app} > g_{leak}(V_\theta - V_{leak}) \ .$$

Between spike events the membrane potential relaxes exponentially from V_{reset} toward V_{SS},

$$V(t) = V_{SS} + (V_{reset} - V_{SS})e^{-t/\tau} \ ,$$

where τ is the relaxation time-constant of the membrane potential. Setting $V(0) = V_{reset}$ and $V(T) = V_\theta$ in this expression one can derive the current-frequency relation

$$f = \frac{1}{T} = \left[-\tau ln\left[\frac{V_\theta - V_{SS}}{V_{reset} - V_{SS}}\right]\right]^{-1}$$

In order to realistically apply IF-style modeling to a pair of interacting neurons, consider the consequences of adding an inhibitory synaptic conductance to Eq. 5 such as the GABA receptor-mediated synaptic conductance of TC cells that is activated by RE cell spiking,

$$C\frac{dV}{dt} = I_{app} - g_{leak}(V - V_{leak}) - g_G(V - V_G) \ . \tag{6}$$

In this case the synaptic conductance, g_G, changes in reaction to incoming action potentials. It is composed of two factors, a dynamic variable, s_G, and a proportionality constant, G_G, with units of $ms \cdot \mu\mathrm{S}/cm^2$ that indicates the synaptic strength.

$$g_G = G_G s_G$$

For physiological accuracy the time course of the gating variable s after a spike evolves according to a function of the form,

$$s(t) = \alpha^2 t e^{-\alpha t}$$

known to computational neuroscientists as an α-function. Such a function can be generated by integrating a second-order differential equation or by integrating two, coupled first-order differential equations such as,

$$\frac{1}{\alpha_G}\frac{ds_G^x}{dt} = -s_G^x \tag{7}$$

and

$$\frac{1}{\alpha_G}\frac{ds_G^y}{dt} = s_G^x - s_G^y \tag{8}$$

and incrementing s_G^x by 1 every time the presynaptic neuron fires, that is,

$$s_G^x(t^-) \rightarrow s_G^x(t^+) + 1$$

The IF model is considerably more minimal than the HH model since it outputs uniform, generic action potentials. However, for some applications this may be acceptable or even preferred. Recall that our primary goal for a model is the accurate production of the frequency of action potentials in a TC-RE network, and thus an IF model is a good starting point.

Firing Rate Models

Just as the IF model did away with certain ionic conductances and simplified the action potenial, firing-rate (FR) models do away with individual action potentials entirely. Instead, it is the frequency of output action potentials, i.e., the cell's 'firing rate', that the FR model calculates. An FR model can be derived from either the HH or IF models. For example, notice that Eq. 6 can be written without I_{app} as,

$$C\frac{dV}{dt} = -g_{eff}(V - V_{eff}) \tag{9}$$

where

$$V_{eff} = \frac{g_L V_L + g_G V_G}{g_{eff}}$$

and

$$g_{eff} = g_L + g_G \ .$$

According to the IF model requirements, when V reaches the threshold voltage, V_θ, an action potential is created and the voltage is set back down to V_{reset} instantaneously. So if the voltage reaches V_θ at t_0 and again at t_1 $(t_1 > t_0)$ then $V(t_0^+) = V_{reset}$ and $V(t_1^-) = V_\theta$

For the next step in the derivation, we must first make an important assumption regarding the time-scale of the synaptic gating variable, s_G. We assume that the value of s_G changes slowly enough over one typical action potential period that it is essentially constant. This assumption means that V_{eff} and g_{eff} are also essentially constant over one action potential period. When $V_{eff} \geq V_\theta$, an action potential is fired regularly every T milliseconds and we

can integrate Eq. 9 over one period, T,

$$\begin{aligned} \int_{V_{reset}-V_{eff}}^{V_\theta - V_{eff}} \frac{d(V-V_{eff})}{V-V_{eff}} &= \frac{-g_{eff}}{C}\int_0^T dt \\ \ln\left(\frac{V_\theta - V_{eff}}{V_{reset}-V_{eff}}\right) &= \frac{-g_{eff}}{C}\,T \end{aligned}$$

and since the firing-rate,f, is the inverse of the period,

$$f = \left(\tau \ln\left(\frac{V_{eff}-V_{reset}}{V_{eff}-V_\theta}\right)\right)^{-1} \tag{10}$$

where both f and V_{eff} are functions of the value of the synaptic gating variable, s_G, and

$$\tau = C/g_{eff}\ .$$

Since f^{pre} indicates how often an action potential is fired by a presynaptic neuron, it can take the place of the incrementing condition on s_G^x in Equation 7. To install f^{pre} into the equation, it's value is multiplied by the incrementing parameter, in this case 1, and added to Eq. 7,

$$\frac{1}{\alpha_G}\frac{ds_G^x}{dt} = f^{pre} - s_G^x \tag{11}$$

Equation 8 remains the same. The two s-equations (Eqs. 11 and 8) along with the firing-rate equation (Eq. 10) comprise the full FR model for a neuron with a self-inhibiting GABA synapse. This derivation and model will be referred to later as we form a model for the more complex TC-RE system.

1.4 Research Accomplishments

As part of my senior project I have developed a mathematical model of a single TC-RE neuron pair that includes an excitatory RGC signal to the TC neurons. I have driven the model with realistic retinal ganglion cell signals and determined values for two parameters in the model. The RGC input is the retinal conductance, here assumed to be of the form, $g_{ret} = {}^0g_{ret} + {}^1g_{ret}e^{i2\pi F_{ret}t}$. I varied the RGC input conductance envelope frequency, F_{ret}, and measured the transmission properties (amplitude and phase shift) of the TC output.

My primary results are numerical simulations, but I also attempted to confirm these results with an analytical approximation in a limited parameter regime where the firing frequency is a linear function of the synaptic gating variable.

2 Model Derivation

I chose to use a firing rate model for our computational experiments due to its high computational efficiency. I wanted an efficient model because future research may involve the simultaneous simulation of many neuron pairs.

2.1 Model Development

To derive the FR model for the TC neuron, we begin with the IF current-balance equation,

$$C\frac{dV^{TC}}{dt} = -g_{leak}^{TC}(V^{TC} - V_{leak}^{TC}) - g_{ret}(V^{TC} - V_{ret}) - g_G(V^{TC} - V_G) \tag{12}$$

The right side includes a retinal conductance, $g_{ret}(t)$, a dynamic GABAergic synaptic conductance, g_G(ultimately a function of the RE neuron firing rate, f^{RE}), and a constant leakage conductance, g_{leak}^{TC}. Following the methods presented in the previous section, Eq. 12 simplifies to,

$$C\frac{dV^{TC}}{dt} = -g_{eff}^{TC}(V^{TC} - V_{eff}^{TC}) \tag{13}$$

where

$$\begin{aligned} V_{eff}^{TC} &= \frac{g_{leak}^{TC}V_{leak}^{TC} + g_{ret}V_{ret} + g_G V_G}{g_{eff}^{TC}}, \\ g_{eff}^{TC} &= g_{leak}^{TC} + g_{ret} + g_G, \end{aligned}$$

and

$$g_G = G_G s_G \ .$$

Integrating Eq. 13 over one period, T, we find the firing-rate of the TC neuron, f^{TC},

$$f^{TC}(g_{ret}, g_G) = \left(\tau^{TC} \ln\left(\frac{V_{eff}^{TC} - V_{reset}^{TC}}{V_{eff}^{TC} - V_{\theta}^{TC}}\right)\right)^{-1} \tag{14}$$

where

$$\tau^{TC} = C/g_{eff}^{TC}$$

Equation 14 is the FR equation for the TC neuron. In the case of the RE neuron, the initial IF current-balance equation is,

$$C\frac{dV^{RE}}{dt} = -g_{eff}^{RE}(V^{RE} - V_{eff}^{RE})$$

and the final FR equation follows similarly,

$$f^{RE}(g_A) = \left(\tau^{RE} \ln\left(\frac{V_{eff}^{RE} - V_{reset}^{RE}}{V_{eff}^{RE} - V_{\theta}^{RE}}\right)\right)^{-1} \tag{15}$$

where,

$$\begin{aligned} \tau^{RE} &= C/g_{eff}^{RE} \ , \\ g_{eff}^{RE} &= g_{leak}^{RE} + g_A \ , \end{aligned}$$

and

$$V_{eff}^{RE} = \frac{g_{leak}^{RE} V_{leak}^{RE} + g_A V_A}{g_{eff}^{RE}} \ .$$

In this model, TC neurons receive excitatory input from the RGC through the retinal conductance, g_{ret}. When the TC neurons fire action potentials they are received by both the RE neurons and V1 of the cortex. The RE neurons receive the TC input through excitatory AMPA receptors. When RE neurons fire, the TC neurons are inhibited through GABA receptors (See Fig. 2). Thus, synaptic gating variables evolve according to,

$$\frac{1}{\alpha_A}\frac{ds_A^x}{dt} = f^{TC} - s_A^x \tag{16}$$

$$\frac{1}{\alpha_A}\frac{ds_A^y}{dt} = s_A^x - s_A^y \tag{17}$$

$$\frac{1}{\alpha_G}\frac{ds_G^x}{dt} = f^{RE} - s_G^x \tag{18}$$

$$\frac{1}{\alpha_G}\frac{ds_G^y}{dt} = s_G^x - s_G^y \tag{19}$$

Eqs. 14, 15, 16–19 compose the FR model of the RE-TC interaction used in the simulations presented later.

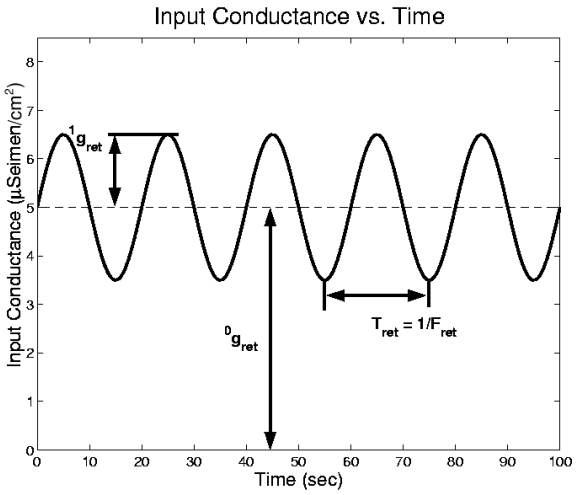

Figure 3: Example of the oscillatory driving retinal conductance used in TC-RE network simulations. In this case the DC amplitude is 5.0 μS/cm^2, the AC amplitude is 1.5 μS/cm^2 and the frequency is 0.05 Hz.

2.2 Retinal Input to the TC-RE Network

Drifting gratings have been commonly used for visual stimulus in neurophysiological experiments for decades [5]. For that reason, we chose a functional form for the retinal conductance, g_{ret}, similar to the firing rate of RGCs under a drifting grating stimulus,

$$g_{ret}(t) = {}^0g_{ret} + {}^1g_{ret}e^{i\omega t} \tag{20}$$

where,

$$\omega = 2\pi F_{ret},$$

$i = \sqrt{-1}$, ${}^0g_{ret}$ is the base conductance amplitude, or DC amplitude, ${}^1g_{ret}$ is the modulating conductance amplitude, or AC amplitude, and F_{ret} is the frequency of oscillation (see Figure 3).

3 Numerical Analysis of Firing-Rate Model

3.1 The Numerical Test

The firing-rate model is a nonlinear system of ordinary differential equations that cannot be solved analytically, so to produce simulation results I used the numerical differential equation solver XPP (X Phase Plane), written by Bard Ermentrout [2]. This program was run interactively after constructing an ASCII input file defining the ordinary differential equations to be integrated. To perform parameter studies, XPP was run repetively in a non-interactive mode. File handling and parameter substitutions were performed using BASH scripts running on a LINUX operating system.

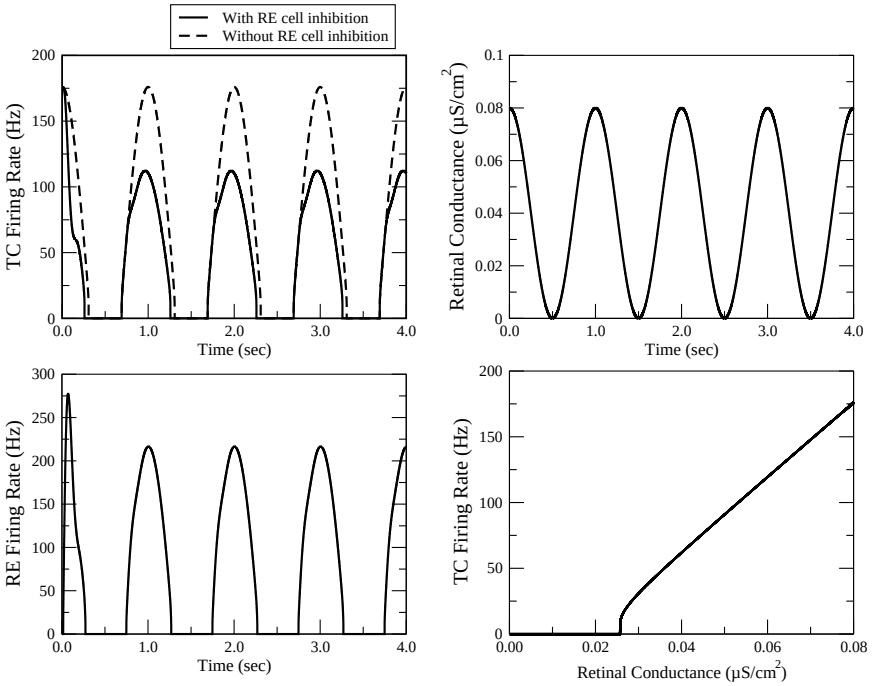

Figure 4: Simulation results produced by an interactive XPP run of the firing-rate model. Top-left: Responses with and without RE cell inhibition of the TC cell. Bottom-left: Response of the RE cell 'follow' the TC cell activity. Top-right: The 1 Hz oscillatory retinal input, g_{ret}. Bottom-right: The TC-response as a function of retinal conductance in the absence of inhibition from RE cells, referred to as a conductance–firing-rate, or g_{ret}-f^{TC}, relation. Parameters: ${}^0g_{ret} = 0.04$ μS, ${}^1g_{ret} = 0.04$ μS, $F_{ret} = 1$ Hz, and as in Table 1.

Figure 4 contains plots produced by using XPP interactively. The system's oscillatory input signal (g_{ret}) is plotted in the top-right pane. The responses of the TC and RE neurons are clearly oscillating at the same frequency as g_{ret}. During the initial half-pulse ($0 \geq t \geq 0.5$ sec) the neuron responses are under the influence of 'transient' effects. Transient fluctuations occur as the system adjusts from user-defined initial conditions to the system's periodic steady state. In this case, the effect only lasts for part of a period, but at higher F_{ret} frequencies, the effects can last many periods.

Though oscillating in unison, the neuron responses differ in the timing of pulse onsets and peaks. Predictably, the onset of RE pulses is after the onset of TC pulses. The amplitude and shape of the TC response changes dramatically when inhibition is applied. The change in amplitude is due to the general action potential-suppressing effect of inhibition, but the shape change is not so easily understood. It results from the RE response offset, and is discussed later. The bottom-right pane of Fig. 4 shows how f^{TC} responds to the retinal conductance value, g_{ret}, when inhibition is not present. As you can see, the neuron does not respond until a certain conductance is reached ($g_{ret} \sim 0.026\ \mu\text{S}/cm^2$). Once above the critical conductance, the firing-rate starts at 0 Hz, moves through a short, almost vertical rise and then relaxes to a trajectory that appears to be linear. The ability for this neuron to fire at infinitely small rates makes it a 'type 1' neuron. ('Type 2' neurons jump to a finite firing rate as soon as the critical conductance is reached).

3.2 Parameter Determination

Because the synaptic conductances g_A, g_G and g_{ret} are difficult to determine directly from experimental literature, reasonable values were selected, based on the physiologically reasonable firing-rates they produce, before performing the parameter studies. The background firing rate of TC cells is 30-40 Hz and 10-20 Hz for RE cells [8, 9]. These background firing rates result from spontaneous retinal activity occuring when there is no visual stimulus (e.g. a gray, monochrome wall). The values of f^{TC} and f^{RE} can range from 0 Hz to well above the

background rates, but it is convenient to fit the parameters to these spontaneous frequencies. First I chose g_{ret} to produce the background f^{TC} value ($g_{ret} \approx 0.032\ \mu\text{S}/cm^2$). Subsequently, g_A and g_G were chosen to produce the backgroud f^{RE} value ($G_A = 0.85\ ms \cdot \mu\text{S}/cm^2$ and $G_G = 0.10\ ms \cdot \mu\text{S}/cm^2$). Values of all other parameters used in the model were taken from Smith et al. 2001 and Smith et al. 2000 and can be found in the Table 1 (see Appendix).

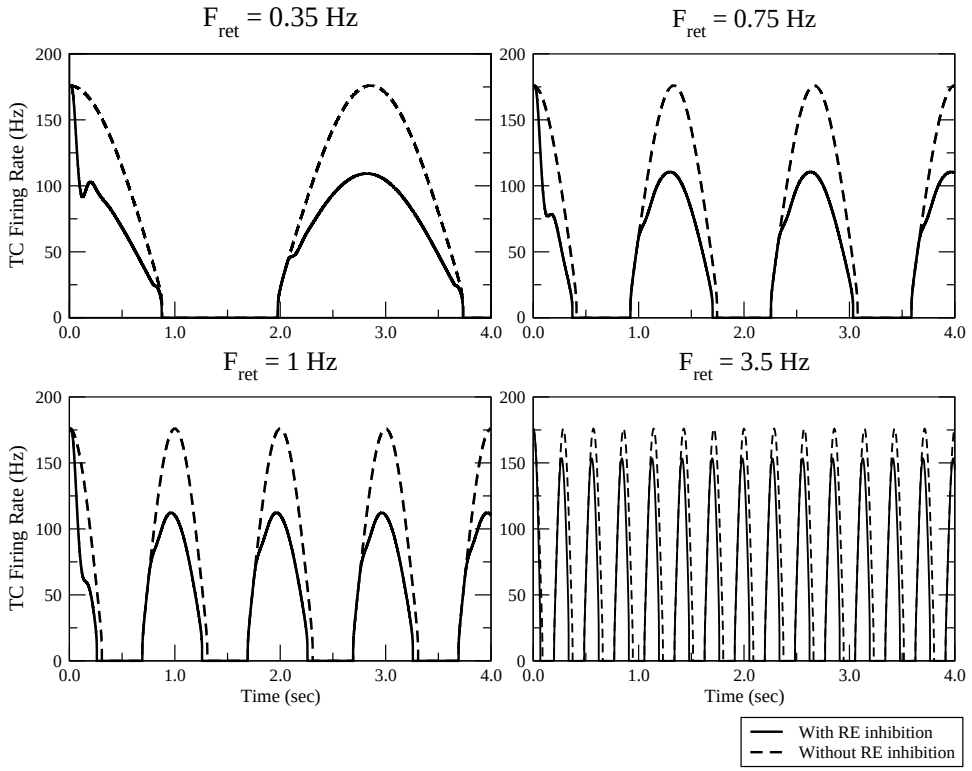

Figure 5: The response of the TC-RE network with four different frequencies of the sinusoidal retinal input, F_{ret}. As in Fig. 4 responses with and without inhibition are plotted. Notice the maximum TC cell firing rate is dependent on F_{ret}. Parameters: ${}^0g_{ret} = 0.04\ \mu$S, ${}^1g_{ret} = 0.04\ \mu$S, and as in Table 1 (see Appendix).

3.3 Numerical Analysis

The primary goal of my research was to determine how RE inhibition modifies the TC firing rate over a range of F_{ret} frequencies. In Fig. 5, the response of the model TC cell is plotted for four values of F_{ret}. As expected, we find that the TC cell firing-rate is reduced by the presence

of inhibitory feedback from RE cells (compare solid and dotted lines) using input conductances identical to Fig. 4. Though the amplitude of the input remains constant throughout the figure, these calculations show that the TC firing rate is dependent on the retinal input envelope frequency, F_{ret} (compare $F_{ret} = 1.0$ Hz and $F_{ret} = 3.5$ Hz). Interestingly, the peak TC firing rate shifts backward in time for all four plotted F_{ret} values under the influence of inhibition. This phenomenon, known as phase advance, has also been observed in FR models that include hyperpolarizing adaption currents [7].

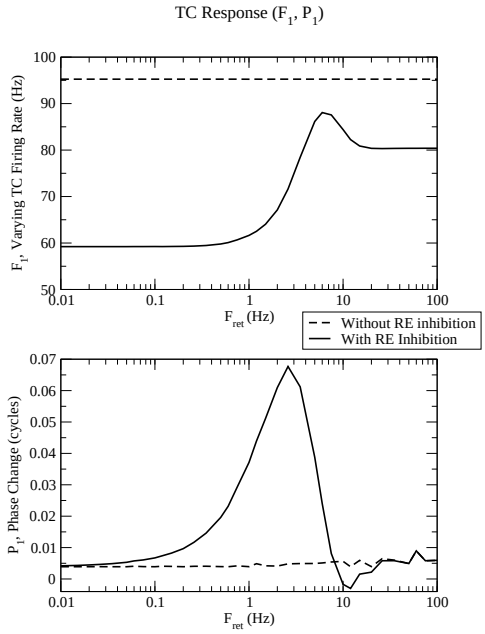

Figure 6: Bode plots summarizing the transmission properties of the TC-RE model. Top: Fourier fundemental, F_1. Bottom: The phase of the Fourier fundemental, P_1. Notice the 'high-pass' character of TC cell response in the presence of RE cell inhibition. Both phase advance and phase delay are observed, depending on the frequency. Parameters: ${}^0g_{ret} = 0.04$ μS, ${}^1g_{ret} = 0.04$ μS, and as in Table 1.

To view the variations in f^{TC} over a large range of F_{ret} values, I wrote a BASH script entitled 'full_FR_ext5'. This script runs a set of XPP simulations in which F_{ret} is varied logarithmically over the range 0.01 Hz - 100 Hz for a total of 37 trials. Data is not kept from the first few periods since 'transient' effects can change the results early in a simulation. The script ensures that once each simulation has passed its transient period, an integer number of cycles is calculated and saved before the simulation ends. More than one cycle of data is saved to reduce variations caused by subharmonics that were sometimes observed for large F_{ret} values. For each F_{ret} value the TC cell response (f^{TC}) was averaged and a discrete Fourier transform (DFT) was performed using an awk script that returns the real-valued amplitude of the first

two Fourier coefficients (F_0 and F_1) and the phase (P_1) of the Fourier fundemental, F_1. These values measure the most important features of each simulation results. The F_0 value is the DC amplitude of the TC cell firing-rate, the F_1 value is the AC amplitude, and P_1 is the phase of the TC cell firing-rate with respect to the retinal input, $g_{ret}(t)$. Plots summarizing these measures – F_0, F_1 and P_1 – as a function of frequency, F_{ret} are called Bode plots.

When given the same input parameters as Figs. 4 and 5, the BASH script full_FR_ext5 produces the Bode plots shown in Fig. 6. The F_1 behavior can be described as a high-pass filter whose transition is mediated by a band-pass filter (see upper pane of Fig 6). The high-pass filter allows signals of F_{ret} >10 Hz to pass with a greater AC amplitude than those of F_{ret} <1 Hz. The band-pass filter allows signals with F_{ret} values near 6 Hz to pass with greater AC amplitudes than any other signals, allowing signals at 6 Hz the strongest transmission. The behavior of the phase over F_{ret} shows an increase of P_1, a phase advance, that rapidly abates at $F_{ret} \sim 4$ Hz, entering a short period of phase delay (see lower pane of Fig 6).

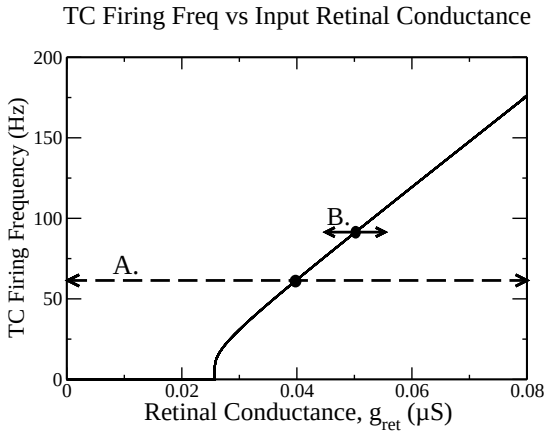

Figure 7: The effect of large AC amplitude (A) compared to small AC amplitude (B). Each arrow shows the range of g_{ret} for that set of parameters. Filled circles indicate the ${}^0g_{ret}$ values. In the case of A, ${}^0g_{ret} = 0.04$ μS, ${}^1g_{ret} = 0.04$ μS, while in the case of B, ${}^0g_{ret} = 0.05$ μS, ${}^1g_{ret} = 0.005$ μS. In the first parameter regime, the large AC amplitude causes the TC firing rate to reach zero. However, when the AC amplitude is small, the TC firing rate remains in the linear region of f^{TC}. (Other parameters as in Table 1.)

All the numerical results reported thus far have the same input conductance values, ${}^0g_{ret} = 0.04$ μS and ${}^1g_{ret} = 0.04$ μS. These values result in TC cell firing rate (f^{TC}) with DC amplitude $F_0 \approx 40$ Hz and AC amplitude, 60 Hz $\leq F_1 \leq 90$ Hz. Figure 7 plots the g_{ret}-f^{TC} relation seen in Fig. 4, highlighting the re-

gions the TC response covers under two sets of retinal conductance values. It is important to notice that the value of ${}^1g_{ret} = 0.04$ μS is large in the sense that ${}^1g_{ret} > {}^0g_{ret}$ or ${}^1g_{ret} \approx {}^0g_{ret}$ implies f^{TC} will reach 0 Hz, passing through a highly non-linear region of the g_{ret}-f^{TC} relation (case A in Fig. 7). Conversely, if ${}^1g_{ret} << {}^0g_{ret}$, the TC cell firing rate will be non-zero throughout the stimulus cycle, remaining in the linear region of the g_{ret}-f^{TC} relation (case B in Fig. 7). In Fig. 7 case A clearly passes through the nonlinear region of the f^{TC} response, while in case B f^{TC} values remain non-zero and within the linear region.

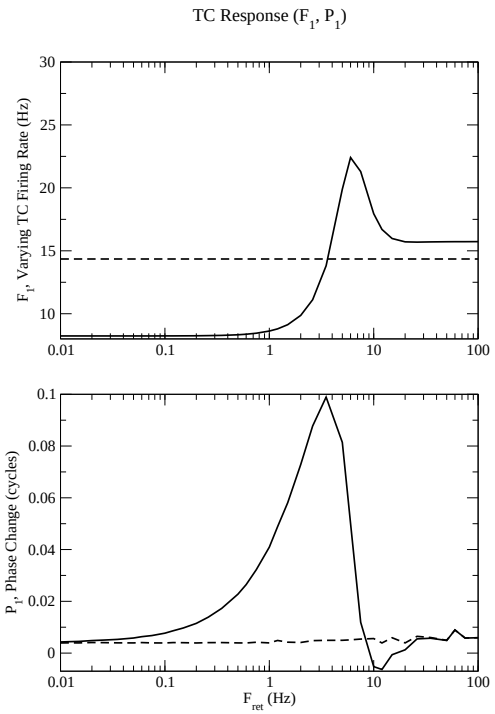

Figure 8: Bode plots for a parameter set idential to case B of Fig. 7, ${}^0g_{ret} = 0.05$ μS, ${}^1g_{ret} = 0.005$ μS. The upper plot is of the F_1 variable and the lower plot is of the phase. (Other parameters as in Table 1.)

In Figure 8, where ${}^0g_{ret} = 0.05$ μS and ${}^1g_{ret} = 0.005$ μS, we can see how the network responds to a smaller ${}^1g_{ret}$ amplitude. This parameter set is identical to that of case B in Fig. 7. Interestingly, the Bode plots are very similar in quality to those of Fig. 6 even though the f^{TC} response no longer travels through the non-linear region of the g_{ret}-f^{TC} curve. The phase change, P_1, does not vary from one ${}^1g_{ret}$ amplitude to the next, except that the peak is about 0.07 cycles when ${}^1g_{ret} = 0.04$ μS and 0.10 cycles when ${}^1g_{ret} = 0.005$ μS. The F_1 response is affected more noticeably by a different ${}^1g_{ret}$. The smaller ${}^1g_{ret}$ of Fig. 8 produces a greater relative leap in F_1 amplitude when comparing the high and low steps of the high-pass filter. The F_1 amplitude increases 100% while Fig. 6 shows an increase in F_1 of about 30%. Similarly, the band-pass filter causes a greater relative amplitude change for the smaller ${}^1g_{ret}$ value. The

F_{ret} value at which the high-pass transition and band-pass filter occur is also approximately the same between the two ${}^{1}g_{ret}$ values.

4 Linearization Approximation of Firing-Rate Model

4.1 Linearization

The firing-rate model described above is complex and non-linear, but it can be simplified by noticing that the dependence of f^{TC} on g_{ret} becomes linear as g_{ret} is increased (bottom-right plot of Fig. 4). If the retinal input $({}^0g_{ret},\ {}^1g_{ret})$ is such that the system is in this 'linear regime' (e.g. case B. of Fig. 7), we can make analytical predictions about retinogeniculate transmission. As with the numerical analysis, the input is a constant-frequency sine-wave with a positive mean (see Fig. 3) but to be in the linear regime we restrict consideration to the case where ${}^0g_{ret} >> {}^1g_{ret}$. Our objective is to derive the system's transmission properties $(F_0,\ F_1,\ P_1)$ from an analytical calculation of f^{TC}. That is, we wish to obtain formulas for F_0, F_1 and P_1 in terms of F_{ret} using the fact that in the linear regime the frequency of the output will be identical to the input frequency (F_{ret}).

First, I derive the general linearized system. This process begins by linearizing the equations for f^{TC} and f^{RE} with respect to g_{ret}, s_G^y and s_A^y. A first-order Taylor expansion of the equations about a set point $(\bar{g}_{ret},\ \bar{g}_G,\ \bar{g}_A)$ gives:

$$f_{lin}^{TC}(\bar{g}_{ret}+\delta g_{ret}, \bar{g}_G+\delta g_G) = f^{TC}(\bar{g}_{ret}, \bar{g}_G) + \left.\frac{\partial f^{TC}}{\partial g_{ret}}\right|_{\bar{g}_{ret},\bar{g}_G} \delta g_{ret} + \left.\frac{\partial f^{TC}}{\partial g_G}\right|_{\bar{g}_{ret},\bar{g}_G} \delta g_G \quad (21)$$

$$f_{lin}^{RE}(\bar{g}_A+\delta g_A) = f^{RE}(\bar{g}_A) + \left.\frac{\partial f^{RE}}{\partial g_A}\right|_{\bar{g}_A} \delta g_A \quad (22)$$

where $\delta g_G = g_G - \bar{g}_G$, and similarly for g_A and g_{ret}.

Next, Eqs. 21 and 22 are rearranged to emphasize the linearity of these new equations:

$$f_{lin}^{TC} = k_0^{TC} + k_I^{TC} s_G^y + k_E^{TC} g_{ret} \quad (23)$$

$$f_{lin}^{RE} = k_0^{RE} + k_E^{RE} s_A^y \quad (24)$$

where k_0, k_I, and k_E are constants (I=inhibitory input, E=excitatory input) given by

$$k_I^{TC} = \left.\frac{\partial f^{TC}}{\partial g_G}\right|_{\bar{g}_G} \quad (25)$$

$$k_E^{TC} = \left.\frac{\partial f^{TC}}{\partial g_{ret}}\right|_{\bar{g}_{ret}} \quad (26)$$

$$
\begin{aligned}
k_0^{TC} &= f^{TC}(\bar{g}_{ret}, \bar{g}_G) - \left.\frac{\partial f^{TC}}{\partial g_{ret}}\right|_{\bar{g}_{ret},\bar{g}_G} \bar{g}_{ret} - \left.\frac{\partial f^{TC}}{\partial g_G}\right|_{\bar{g}_{ret},\bar{g}_G} \bar{g}_G \qquad (27)\\
k_E^{RE} &= \left.\frac{\partial f^{RE}}{\partial g_A}\right|_{\bar{g}_A}\\
k_0^{RE} &= f^{RE}(\bar{g}_A) + \left.\frac{\partial f^{RE}}{\partial g_A}\right|_{\bar{g}_A} \bar{g}_A
\end{aligned}
$$

Each of the partial derivatives above has been calculated and is a function of the parameters of the original firing-rate model and the chosen set point (see Appendix). Using Eqs. 23 and 24 and substituting for f^{TC} and f^{RE} in Eqs. 16–19 gives the linearized dynamics of the synaptic gating variables:

$$
\frac{d}{dt}\begin{bmatrix} s_A^x \\ s_A^y \\ s_G^x \\ s_G^y \end{bmatrix} = \begin{bmatrix} -\alpha_A & 0 & 0 & \alpha_A k_I^{TC} \\ \alpha_A & -\alpha_A & 0 & 0 \\ 0 & \alpha_G k_E^{RE} & -\alpha_G & 0 \\ 0 & 0 & \alpha_G & -\alpha_G \end{bmatrix} \begin{bmatrix} s_A^x \\ s_A^y \\ s_G^x \\ s_G^y \end{bmatrix} + \begin{bmatrix} \alpha_A(k_0^{TC} + k_E^{TC} g_{ret}) \\ 0 \\ \alpha_G k_0^{RE} \\ 0 \end{bmatrix}
$$

Substituting a solution of this system into Eqs. 23 and 24 yields a solution of the linearized firing-rate model. Next, we perform linear systems analysis and assume that all the synaptic variables and the resulting firing rates include both an AC and DC component similar to the retinal input (Eq. 20). Thus, Eqs. 23 and 24 take the form,

$$
\begin{aligned}
{}^0 f_{lin}^{TC} + {}^1 f_{lin}^{TC} e^{i\omega t} &= k_0^{TC} + k_I^{TC}({}^0 s_G^y + {}^1 s_G^y e^{i\omega t}) + k_E^{TC}({}^0 g_{ret} + {}^1 g_{ret} e^{i\omega t})\\
{}^0 f_{lin}^{RE} + {}^1 f_{lin}^{RE} e^{i\omega t} &= k_0^{RE} + k_E^{RE}({}^0 s_A^y + {}^1 s_A^y e^{i\omega t})
\end{aligned}
$$

and the dynamics of the synaptic gating variables is given by,

$$\frac{d}{dt}\begin{bmatrix} {}^0s_A^x + {}^1s_A^x e^{i\omega t} \\ {}^0s_A^y + {}^1s_A^y e^{i\omega t} \\ {}^0s_G^x + {}^1s_G^x e^{i\omega t} \\ {}^0s_G^y + {}^1s_G^y e^{i\omega t} \end{bmatrix} = \begin{bmatrix} -\alpha_A & 0 & 0 & \alpha_A k_I^{TC} \\ \alpha_A & -\alpha_A & 0 & 0 \\ 0 & \alpha_G k_E^{RE} & -\alpha_G & 0 \\ 0 & 0 & \alpha_G & -\alpha_G \end{bmatrix} \begin{bmatrix} {}^0s_A^x + {}^1s_A^x e^{i\omega t} \\ {}^0s_A^y + {}^1s_A^y e^{i\omega t} \\ {}^0s_G^x + {}^1s_G^x e^{i\omega t} \\ {}^0s_G^y + {}^1s_G^y e^{i\omega t} \end{bmatrix}$$

$$+ \begin{bmatrix} \alpha_A \left[k_0^{TC} + k_E^{TC}({}^0g_{ret} + {}^1g_{ret} e^{i\omega t}) \right] \\ 0 \\ \alpha_G k_0^{RE} \\ 0 \end{bmatrix} \tag{28}$$

Taking the time derivative on the LHS of Eq. 28, this linear system can be separated into two independent systems, one whose terms involve $e^{i\omega t}$ and is oscillatory and the other which is not (the AC and DC systems, respectively). The DC system is,

$$ {}^0f_{lin}^{TC} = k_0^{TC} + k_I^{TC}\ {}^0s_G^y + k_E^{TC}\ {}^0g_{ret} \tag{29}$$

$$ {}^0f_{lin}^{RE} = k_0^{RE} + k_E^{RE}\ {}^0s_A^y \tag{30}$$

where,

$$\begin{bmatrix} {}^0s_A^x \\ {}^0s_A^y \\ {}^0s_G^x \\ {}^0s_G^y \end{bmatrix} = \begin{bmatrix} -\alpha_A & 0 & 0 & \alpha_A k_I^{TC} \\ \alpha_A & -\alpha_A & 0 & 0 \\ 0 & \alpha_G k_E^{RE} & -\alpha_G & 0 \\ 0 & 0 & \alpha_G & -\alpha_G \end{bmatrix} \begin{bmatrix} {}^0s_A^x \\ {}^0s_A^y \\ {}^0s_G^x \\ {}^0s_G^y \end{bmatrix} + \begin{bmatrix} \alpha_A(k_0^{TC} + k_E^{TC}\ {}^0g_{ret}) \\ 0 \\ \alpha_G k_0^{RE} \\ 0 \end{bmatrix}$$

After dropping the factors of $e^{i\omega t}$ that affect every term, the AC system is,

$$ {}^1f_{lin}^{TC} = k_I^{TC}\ {}^1s_G^y + k_E^{TC}\ {}^1g_{ret} \tag{31}$$

$$ {}^1f_{lin}^{RE} = k_E^{RE}\ {}^1s_A^y \tag{32}$$

where,

$$i\omega \begin{bmatrix} {}^1s_A^x \\ {}^1s_A^y \\ {}^1s_G^x \\ {}^1s_G^y \end{bmatrix} = \begin{bmatrix} -\alpha_A & 0 & 0 & \alpha_A k_I^{TC} \\ \alpha_A & -\alpha_A & 0 & 0 \\ 0 & \alpha_G k_E^{RE} & -\alpha_G & 0 \\ 0 & 0 & \alpha_G & -\alpha_G \end{bmatrix} \begin{bmatrix} {}^1s_A^x \\ {}^1s_A^y \\ {}^1s_G^x \\ {}^1s_G^y \end{bmatrix} + \begin{bmatrix} \alpha_A k_E^{TC} {}^1g_{ret} \\ 0 \\ 0 \\ 0 \end{bmatrix}$$

Notice that the transmission properties of the network that are of interest (F_0, F_1, P_1) are easily written in terms of the AC and DC components of the TC cell firing rate, that is,

$$\begin{aligned} F_0 &= |{}^0f_{lin}^{TC}| \\ F_1 &= |{}^1f_{lin}^{TC}| \\ P_1 &= \angle {}^1f_{lin}^{TC} \ . \end{aligned}$$

where $|z|$ is the complex modulus of z and $\angle z$ is the complex argument or angle of z. In order to calculate these response measures analytically in the linear regime, the solutions of the AC and DC synaptic dynamics were derived using the symbolic computer algebra toolbox of Matlab.

The solution of the DC system is,

$$\begin{aligned} {}^0s_A^x &= (k_0^{TC} + k_I^{TC}k_0^{RE} + k_E^{TC}\ {}^0g_{ret})/(1 - k_I^{TC}k_E^{RE}) \\ {}^0s_A^y &= (k_0^{TC} + k_I^{TC}k_0^{RE} + k_E^{TC}\ {}^0g_{ret})/(1 - k_I^{TC}k_E^{RE}) \\ {}^0s_G^x &= (k_0^{RE} + k_E^{RE}k_0^{TC} + k_E^{RE}k_E^{TC}\ {}^0g_{ret})/(1 - k_I^{TC}k_E^{RE}) \\ {}^0s_G^y &= (k_0^{RE} + k_E^{RE}k_0^{TC} + k_E^{RE}k_E^{TC}\ {}^0g_{ret})/(1 - k_I^{TC}k_E^{RE}) \end{aligned} \tag{33}$$

The solution of the AC system is,

$$\begin{aligned} {}^1s_A^x = \ & - \ {}^1g_{ret}k_E^{TC}\alpha_A(\alpha_A + i\omega)(-\alpha_G^2 - 2i\alpha_G\omega + \omega^2) \\ & \times \ (\alpha_A^2\alpha_G^2 + 2i\alpha_A^2\alpha_G\omega - \alpha_A^2\omega^2 + 2i\omega\alpha_A\alpha_G^2 - 4\omega^2\alpha_A\alpha_G - 2i\omega^3\alpha_A - \omega^2\alpha_G^2 \\ & - \ 2i\omega^3\alpha_G + \omega^4 - k_I^{TC}k_E^{RE}\alpha_A^2\alpha_G^2)^{-1} \end{aligned}$$

$$
\begin{aligned}
{}^1s_A^y = \; & - \; {}^1g_{ret} k_E^{TC} \alpha_A^2 (-\alpha_G^2 - 2i\alpha_G\omega + \omega^2) \\
& \times \; (\alpha_A^2\alpha_G^2 + 2i\alpha_A^2\alpha_G\omega - \alpha_A^2\omega^2 + 2i\omega\alpha_A\alpha_G^2 - 4\omega^2\alpha_A\alpha_G - 2i\omega^3\alpha_A - \omega^2\alpha_G^2 \\
& - \; 2i\omega^3\alpha_G + \omega^4 - k_I^{TC} k_E^{RE} \alpha_A^2 \alpha_G^2)^{-1}
\end{aligned}
$$

$$
\begin{aligned}
{}^1s_G^x = \; & i \; {}^1g_{ret} k_E^{TC} k_E^{RE} \alpha_A^2 \alpha_G (\omega - i\alpha_G)(-\alpha_G^2 - 2i\alpha_G\omega + \omega^2) \\
& \times \; (\alpha_A^2\alpha_G^2 + 2i\alpha_A^2\alpha_G\omega - \alpha_A^2\omega^2 + 2i\omega\alpha_A\alpha_G^2 - 4\omega^2\alpha_A\alpha_G - 2i\omega^3\alpha_A - \omega^2\alpha_G^2 \\
& - \; 2i\omega^3\alpha_G + \omega^4 - k_I^{TC} k_E^{RE} \alpha_A^2 \alpha_G^2)^{-1}
\end{aligned} \tag{34}
$$

$$
\begin{aligned}
{}^1s_G^y = \; & \; {}^1g_{ret} k_E^{TC} k_E^{RE} \alpha_A^2 \alpha_G^2 (-\alpha_G^2 - 2i\alpha_G\omega + \omega^2) \\
& \times \; (\alpha_A^2\alpha_G^2 + 2i\alpha_A^2\alpha_G\omega - \alpha_A^2\omega^2 + 2i\omega\alpha_A\alpha_G^2 - 4\omega^2\alpha_A\alpha_G - 2i\omega^3\alpha_A - \omega^2\alpha_G^2 \\
& - \; 2i\omega^3\alpha_G + \omega^4 - k_I^{TC} k_E^{RE} \alpha_A^2 \alpha_G^2)^{-1}
\end{aligned}
$$

Substituting these values into Eqs. 29 and 31 gives the final result.

$$
\begin{aligned}
F_0 &= |{}^0f_{lin}^{TC}| = |k_0^{TC} + k_I^{TC} \; {}^0s_G^y + k_E^{TC} \; {}^0g_{ret}| \\
F_1 &= |{}^1f_{lin}^{TC}| = |k_I^{TC} \; {}^1s_G^y + k_E^{TC} \; {}^1g_{ret}| \\
P_1 &= \angle {}^1f_{lin}^{TC} = \angle (k_I^{TC} \; {}^1s_G^y + k_E^{TC} \; {}^1g_{ret}) \; .
\end{aligned}
$$

where k_0^{TC}, k_I^{TC}, k_E^{TC}, ${}^0s_G^y$, and ${}^1s_G^y$ are given in Eqs. 25–27, 35–45, 33 and 34.

4.2 Results

After deriving the linearized model, I used Matlab to numerically determine the resulting F_1 and P_1 values over F_{ret}. Figure 9 contains Bode plots of the TC cell response of the linearized model. As you can see, the response appears to be very similar to those seen in the numerical modeling (Figs. 6 and 8). The F_1 response exhibits the behavior of a high-pass filter mediated by a band-pass filter. The P_1 response indicates an exponential rise in phase advancing until peaking out around $F_{ret} \approx 4$ Hz and dropping quickly for a brief phase delay that relaxes back to zero phase change.

However, for another retinal DC input parameter, ${}^0g_{ret} = 0.07$ μS, the TC response behavior is quite different. Figure 10 is a plot of the linearized response when ${}^0g_{ret} = 0.07$ μS and ${}^1g_{ret} = 0.005$ μS. While the form of the F_1 response in this parameter regime is the same as before, it is now much more heavily characterized as a band-pass filter than a high-pass filter. The phase response in Fig. 10 is very different from the response seen in Fig. 9. In Fig. 10, the P_1 value increases until it reaches 0.5 cycles then instantaneously falls to -0.5 cycles. Actually, this is not an instantaneous change. The program analyzing the data displays phase shifts in the smallest amount of shift possible, so when the phase advances beyond 0.5 cycles, the program displays the shift as a shorter delay rather than a longer advance. What is truly happening in Fig. 10 is one of two things: a phase advance that carries through a full cycle, or, a phase delay that relaxes up to zero, where the initial P_1 value is -0.8. The latter is the more probable case since it ends on zero phase change, like the previous P_1 behavior we have seen. Also, the strong phase advance case never allows P_1=0, which would also be unlike previous F_1 behavior.

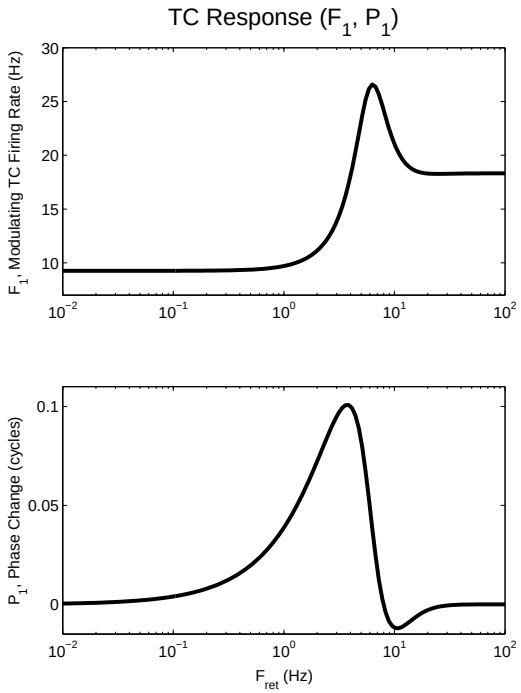

Figure 9: Bode plots of the transmission properties of the linearized TC-RE model. The upper plot is of the F_1 amplitude and the lower plot is of the phase, P_1. These results are an example of the limited success of the linearization. Comparing this case with its numerical counterpart (Fig. 8) reveals the linearization for this parameter regime is in strong agreement. Parameters: ${}^0g_{ret} = 0.05$ μS, ${}^1g_{ret} = 0.005$ μS, and as in Table 1.

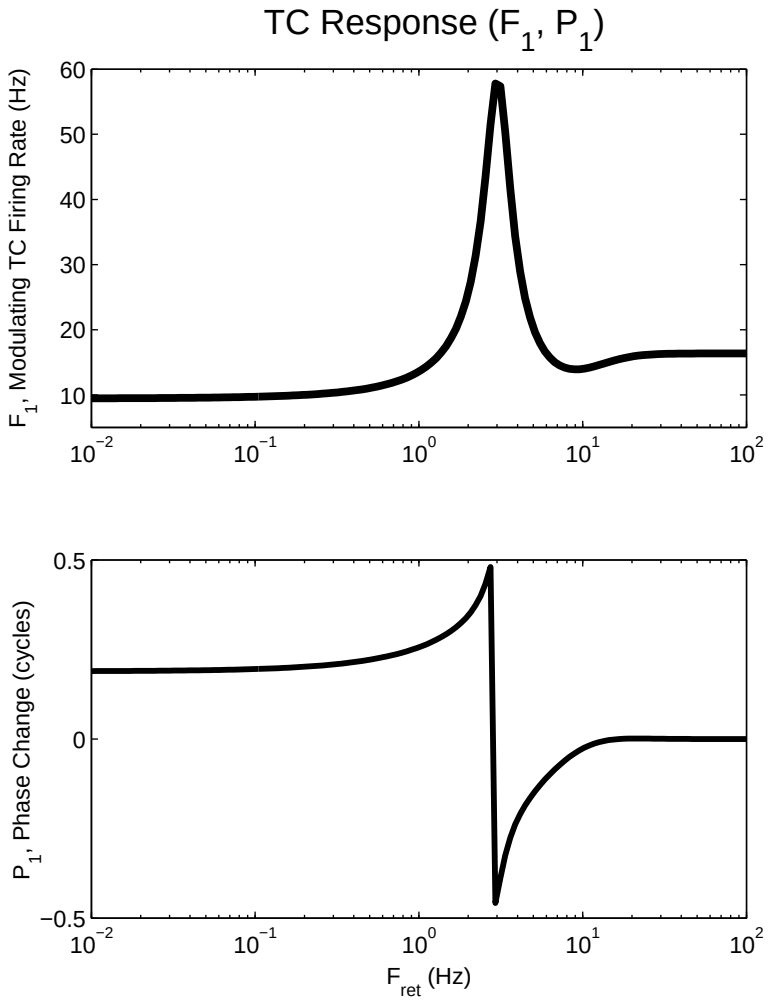

Figure 10: Linearized TC-RE model Bode plots. The upper plot is of the F_1 amplitude and the lower plot is of the phase, P_1. Here you see that the linearization's solution can differ greatly both qualitatively and quantitatively from the numerical results. This fact, along with analysis backing the correctness of the numerical solutions, implies that the linearization was not derived or calculated correctly. Parameters: ${}^0g_{ret} = 0.07$ μS, ${}^1g_{ret} = 0.005$ μS, and as in Table 1.

5 Discussion

5.1 Describing the Results

The numerical analysis gave consistent qualitative results across the parameter scheme I used. As expected, when inhibition is present the F_0 transmission feature was reduced. When the g_{ret} values are in the linear region of the f^{TC} response curve, the reduction of F_0 is independent of F_{ret}. The Bode plots have the same form over a range of retinal input values. The typical behavior of the F_1 response as a function of F_{ret} can be described as a high-pass filter whose transition is mediated by a band-pass filter (see upper pane of Fig. 6). A high-pass filter allows signals of F_{ret} greater than the filter transition value to pass with a greater AC amplitude than those of F_{ret} less than the transition value. In the case of Fig. 6 the transition value is about 5 Hz. In Fig. 6 the filter's minimum value is about 60 Hz and the maximum is about 80 Hz, but as you can see neither reaches the no-inhibition firing frequency ($\sim$95 Hz). The emergence of high-pass filter behavior is an interesting development. This type of filter might suggest that the high frequency input components are more important than the low frequency components for down-stream processes, presumably within the cortex. A band-pass filter allows signals with F_{ret} values near a critical F_{ret} value to pass with greater AC amplitudes than other signals, allowing the critical value the strongest response. In Fig. 6, the band-pass filter is active between 1 Hz and 10 Hz, with the greatest influence around $F_{ret} = 6$ Hz, its critical value. Interestingly, the 'action' of both filters, that is, the location in F_{ret}-space for which the filter changes its transmission properties most dramatically, occurs between 1 and 10 Hz. In other words, both the high-pass filter's transition value and the band-pass filter's critical value fall within $1 < F_{ret} < 10$ Hz.

The usual behavior of the phase over F_{ret} is a gradual rise from low frequencies, followed by a rapid drop, falling slightly below zero, and ending with a relaxation back up to zero, the same value as the lowest F_{ret} produced (see lower pane of Fig 6). (The jagged behavior of the phase at higher F_{ret} values is a numerical artifact. The actual behavior is a relaxation

up to zero). The effect of inhibition on P_1 indicates phase advance for most F_{ret} values. This means the signal's peak is phase-shifted to occur sooner than it would have without inhibition, which can be seen in Fig. 5. The pulses that occur when inhibition is included are smaller and their peaks are slightly left of the pulses that occur without inhibition. The phase shift occurs because the inhibition builds up during the initial active phase of the TC cell response and then suddenly bursts out, dampening the TC firing rate demonstrably. The burst of inhibition lowers the original peak of the TC signal far enough that it actually falls below the value for earlier parts of the TC signal. Thus, an earlier section of the TC signal now becomes the peak.

The phase always reaches its peak value near the same F_{ret} as the steepest positive slope of F_1. In addition, F_1 reaches its peak value as the phase moves through its steepest negative slope. These coincidences are notable since they indicate that there may be a causation between the two transmission measures. Both peaks fall within a region loosely defined as 1 Hz $\leq F_{ret} \leq$ 10 Hz when α_A, $\alpha_G = 0.05\ ms^{-1}$. The fact that the peaks of P_1 and F_1 occur so close together in F_{ret}-space indicates that signals with F_{ret} values of that region are more heavily modified by the presence of RE-inhibition than signals with larger or smaller F_{ret} values (though $F_{ret} > 10$ Hz still receives an amplitude boost). This means that F_{ret} values in that region appear to be selectively affected by reticular cell inhibition. However, crucial factors in determining the F_{ret} range over which the region occurs are the α_A and α_G values, which I reduced from their experimentally determined quantities in my models to reduce a numerical artifact.

5.2 Numerical Results vs. Linearization Results

I performed the linearization of the firing-rate model to test whether the numerical simulations were giving correct results. The linearization is only a valid approximation when ${}^1g_{ret} << {}^0g_{ret}$ and f^{TC} does not pass into the non-linear region of the g_{ret}-f^{TC} relation (such as case B in Fig. 7). I made comparisons of the numerical simulations and analyt-

ical linearization under valid g_{ret} parameters to try to determine whether the numerical simulations were correct, though I eventually decided the analytical results were incorrect.

The first comparison is the most successful one, the numerical simulations of Fig. 8 compared to the analytical answer of Fig. 9. The retinal input parameters for both these solutions are ${}^0g_{ret} = 0.05$ μS and ${}^1g_{ret} = 0.005$ μS. The resulting Bode plots are nearly identical, not only qualitatively, but quantitatively as well. The only discrepancy is a constant difference between the F_1 values of about 2 Hz. When ${}^1g_{ret}$ is changed to 0.01 μS and 0.02 μS, the analytical solution continues to agree very well with numerical results. The only apparent discrepancy is a slowing increasing prominence of the band-pass characteristic of the analytical solution, noticed when comparing the relative amplitudes of the filter characteristics.

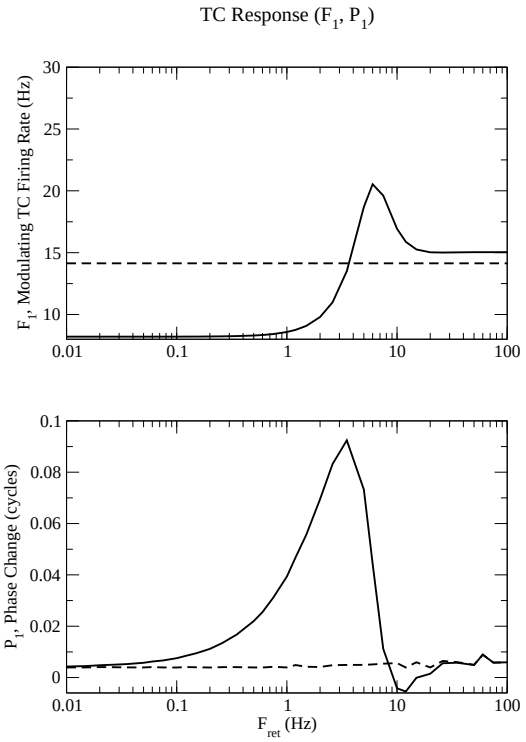

Figure 11: Bode plots of transmission properties of the TC-RE model. The upper plot is of the F_1 amplitude and the lower plot is of the phase, P_1. Comparing these results to the analytical counterparts (Fig. 10) reveals a definite lack of agreement between the two analyses. Parameters: ${}^0g_{ret} = 0.07$ μS, ${}^1g_{ret} = 0.005$ μS, and as in Table 1.

The next comparison is performed after changing the DC retinal input parameter to ${}^0g_{ret} = 0.07$ μS, ${}^1g_{ret}$ remains 0.005 μS. The analytical results (see Fig. 10) were described in the last section. The numerical results are plotted in Fig. 11. Comparing the two figures reveals obvious differences between the results. The main contrast between the F_1 plots is the greatly emphasized prominence of band-pass filter effects in the analytical solution. While that difference causes the two plots to appear very different at

first glance, a closer evaluation reveals that the high-pass filter properties appear to be in as close agreement as with the last comparison. The P_1 responses of the numerical and analytical solutions are only in agreement at large F_{ret}, where both go to zero. The initial, positive section of P_1 in Fig. 10 should be considered a delay (subtract 1 from the values), not an advance, as discussed in the previous section. The long period of phase delaying seen in the analytical solution does not appear in the numerical results. Phase delays due appear in the latter, but not until the phase shift is zero in the former. The general, qualitative shape of the two results do not even agree.

These sorts of differences between the analytical and numerical results are seen as ${}^0g_{ret}$ is set to larger values, the greater the value, the greater the differences. However, as the first paragraph discussed, an increase in ${}^1g_{ret}$ does not cause major discrepancies to appear.

5.3 Problems and Improvements

The disagreement between analytical and numerical results is clearly a problem. I verified the numerical results by reading the F_1 and P_1 values off of the raw data and comparing it to the F_1 and P_1 values plotted in the Bode plots. This method confirmed the correctness of the numerical results. Therefore, I believe the error causing the discrepancies lies in the linearization. Canidates of the error are any of the equation and parameter entries into software and the determination of the k-variables, which was performed manually. Rederiving the k-variables and checking the equation entry into software could solve this problem.

There appears to be a problem in the numerics of the BASH script that causes the P_1 values at large F_{ret} to accumulate some noise (see Fig. 6). The fact that the P_1 values are jagged at large F_{ret} even when there is no inhibition, indicates the likelihood of bad averaging being the culprit.

Many of the problems I encountered during this research concerned producing acceptable Bode plots and understanding how unexpected phenomena occuring in the data could create discrepancies in the plots. There were two particular phenomena of the raw f^{TC} data that

should be kept in mind by anyone reproducing this work. The first is temporal, non-transient subharmonics in f^{TC}. It was common to see subharmonics during the transient period of simulations, but sometimes the subharmonics were permanent. When this occured, I had to increase the number of cycles sampled per F_{ret} considerably. Oftentimes the subharmonics would cycle only after long periods lasting dozens of cycles. Another way to get around the problem of subharmonics is to increase the α-variable values. The second phenomenon seen was ultra-rapid f^{TC} spiking at low g_{ret} values. This occurred frequently when F_{ret} was small. While the subharmonics are a physiologically realistic phenomenon, the ultra-rapid spikes are not, they are numerical artifacts. To avoid them, raise ${}^0g_{ret}$, decrease the α-variable values (which, in turn may lead to stronger subharmonics), or use a small enough dt in numerical calculations to model the spikes accurately so they will average out without creating an offset in f^{TC}. Whenever possible discrepancies appear in the Bode plots it is important to check the raw XPP data to see if the cause is an unwanted artifact or unexpected dynamics.

6 Conclusion

The goal of my research was to determine how reticular inhibition affects retinogeniculate transmission. To accomplish this, I first adapted an integrate-and-fire model of Dr. Smith's to the neuron network I am studying and derived a firing-rate model of a TC-RE pair [7]. Next, I determined approximate values for several undefined model parameters by fitting numerical model results to known firing rates [9]. Then I analyzed the model numerically using the program XPP and, using a BASH script evaluated the behavior of many XPP runs, focusing on changes in response measures (F_0, F_1 and P_1) over a range of retinal input frequencies (F_{ret}).

The Bode plots, resulting from full_FR_ext5, agree very well with the raw XPP output. That correlation implies the discrete Fourier transform script is correctly calculating the transmission properties. Therefore, we have reason to believe that the Bode plots are accurate descriptions of the system defined by the FR model. To further convince myself of the model's viability I undertook a more analytical analysis of the FR model. The system of equations is too complex to solve analytically, so I chose the approximation method of linearization about a fixed point. The results of the linearization agree strongly with the numerical results over a limited range of retinal input, however, the two models to do not agree well enough to consider the linearization successful.

Numerical analysis brought forward some interesting transmission properties of the model. Among them, the regularity of temporal signal phase-advancing. Also of note was the high-pass filter characteristic of the amplitude-modifying property (F_1) of the network and its band-pass filter mediator. The close proximity of the F_1 and P_1 peaks is of interest because it implies that retinal ganglion cell signals of a certain F_{ret} range may be selectively affected by the reticular cell inhibition when transferred by the thalamocortical cells. The high-pass filter is the most interesting characteristic of the transmission because it indicates that incoming signals will have their high frequency components transferred better than the low frequency components, which implies that the high frequency components may be more

important for cortical processes.

Appendix

Firing-Rate Model Parameter Values:

Table 1: Model parameter values [7, 6]

Parameter	Value
G_A	0.85 ms·μS/cm^2
G_G	0.10 ms·μS/cm^2
α_A	0.05 ms^{-1}
α_G	0.05 ms^{-1}
C	1 μF/cm^2
g_{leak}^{TC}	0.03 μS/cm^2
g_{leak}^{RE}	0.03 μS/cm^2
V_{leak}^{TC}	-65 mV
V_{leak}^{RE}	-65 mV
V_{θ}^{TC}	-35 mV
V_{θ}^{RE}	-35 mV
V_{reset}^{TC}	-50 mV
V_{reset}^{RE}	-50 mV
V_G	-85 mV
V_A	0 mV
V_{ret}	0 mV

Linearization k-variable components:

$$\frac{\partial f^{TC}}{\partial g_G} = \frac{\partial f^{TC}}{\partial V_{eff}^{TC}} \frac{\partial V_{eff}^{TC}}{\partial g_G} + \frac{\partial f^{TC}}{\partial \tau^{TC}} \frac{\partial \tau^{TC}}{\partial g_G} \tag{35}$$

$$\frac{\partial f^{TC}}{\partial g_{ret}} = \frac{\partial f^{TC}}{\partial V_{eff}^{TC}} \frac{\partial V_{eff}^{TC}}{\partial g_{ret}} + \frac{\partial f^{TC}}{\partial \tau^{TC}} \frac{\partial \tau^{TC}}{\partial g_{ret}} \tag{36}$$

$$\frac{\partial f^{RE}}{\partial g_A} = \frac{\partial f^{RE}}{\partial V_{eff}^{RE}} \frac{\partial V_{eff}^{RE}}{\partial g_A} + \frac{\partial f^{RE}}{\partial \tau^{RE}} \frac{\partial \tau^{RE}}{\partial g_A} \tag{37}$$

where,

$$\frac{\partial f^{TC}}{\partial V_{eff}^{TC}} = -{f^{TC}}^2 \tau^{TC} \left[\frac{V_{reset}^{TC} - V_{\theta}^{TC}}{(V_{eff}^{TC} - V_{reset}^{TC})(V_{eff}^{TC} - V_{\theta}^{TC})} \right] \tag{38}$$

$$\frac{\partial V_{eff}^{TC}}{\partial g_G} = \frac{g_{leak}^{TC}(V_G - V_{leak}^{TC}) + g_{ret}(V_G - V_{ret})}{(g_{leak}^{TC} + g_{ret} + g_G)^2} \tag{39}$$

$$\frac{\partial f^{TC}}{\partial \tau^{TC}} = -{f^{TC}}^2 ln \left[\frac{V_{eff}^{TC} - V_{reset}^{TC}}{(V_{eff}^{TC} - V_{\theta}^{TC})} \right] \tag{40}$$

$$\frac{\partial \tau^{TC}}{\partial g_G} = -C(g_{leak}^{TC} + g_{ret} + g_G)^{-2} \tag{41}$$

$$\frac{\partial V_{eff}^{TC}}{\partial g_{ret}} = \frac{g_{leak}^{TC}(V_{ret} - V_{leak}^{TC}) + g_G(V_{ret} - V_G)}{(g_{leak}^{TC} + g_{ret} + g_G)^2} \tag{42}$$

$$\frac{\partial \tau^{TC}}{\partial g_{ret}} = -C(g_{leak}^{TC} + g_{ret} + g_G)^{-2} \tag{43}$$

$$\frac{\partial V_{eff}^{RE}}{\partial g_A} = \frac{g_{leak}^{RE}(V_A - V_{leak}^{RE})}{(g_{leak}^{RE} + g_A)^2} \tag{44}$$

$$\frac{\partial \tau^{RE}}{\partial g_A} = -C(g_{leak}^{RE} + g_A)^{-2} \tag{45}$$

Code of 'full_FR_ext5':

```
#  THis script combines data-producing script, 'FR_dyna_dm_alpha', and
#   fourier analysis script, 'four_data_maker', so that all is done at once
.
#   Now  a script section has been added that will draw to 8-frame
#    xmgrace plots, one for the inhibited fouriered data, one for the
#    uninhibited fouriered data.
#  This version (full_FR_ext2) uses the 'freq_to_ttc.awk' file to determine
 the
#     trans, total, and cycles for each freq for XPP runs and 'aver_t.awk'
#     to average multiple cycle data together.
######## Four parameters I might like to vary:       ###################
AC_COND=0.005
DC_COND=0.07
G_AMPA=0.85
G_GABA=0.1
ALPHA_AM=0.05
ALPHA_GA=0.05
##### REMOVING  ALL  FILES  IN  test_out/raw_FR_data !!!!!!!######
rm -r ~/test_out/raw_FR_data/*
rm -f -r ~/test_out/foured/*${AC_COND}_${DC_COND}.dat
rm -f -r ~/test_out/aved/*.*
rm ~/test_out/*.log
declare -a TEST_RATE
declare -a WAVE_LENGTH
declare -a TRANS
declare -a DT
```

```
##the following test rates (for the FR) now cover from .01 Hz to 100 Hz wit
h the div_factor of 1000
## The following values are in milliseconds:
##   (TOTAL_TIME is the wave length + transient)
# new test rates (37 in all):

echo "DC conductance = " $DC_COND >> ~/test_out/test.log

echo "AC conductance = " $AC_COND >> ~/test_out/test.log
echo "AMPA max conductance = " $G_AMPA >> ~/test_out/test.log
echo "GABA max conductance = " $G_GABA >> ~/test_out/test.log
echo "AMPA alpha value = " $ALPHA_AM >> ~/test_out/test.log
echo "GABA alpha value = " $ALPHA_GA >> ~/test_out/test.log

echo "run#  freq   tran_t   tot_t    #cycs" >> ~/test_out/test.log


#wave lengths(msec)=(  100000   83333.33  66666.66  50000.0   38461.5   285
71.4  20000.0  16666.66  13333.33  10000    8333.33  6666.66  5000.0   3846
.15   2857.14  2000.0  1666.666  1333.333  1000.0  833.333  666.666  500.0
  384.615   285.714   200.0   166.666   133.333   100.0   83.3333   66.6666
  50.0   38.4615  28.5714   20.0   16.6666  13.3333   10.0)
          TEST_RATE=(  .01      .012      .015      .02       .026      .03
5     .05      .060      .075      .10      .12      .15      .2       .26
      .35      .5      .6        .75       1.0     1.2      1.5      2.0
  2.6       3.5       5.0     6.0       7.5       10      12        15
```

```
  20      26        35         50      60        75         100)
          DT=(          10        10         9         9          8          6
      5         4          3          2         2         2         2         1
      1         1         1          1          1        .8        .6        .55
  .45        .4         .35      .3         .28         .23       .2        .15
   .1     .08       .07         .06     .05       .035        .03)
          #CYCLES=(      1         1          1          1          2          2
       2         2          2          2         2         2         2         2
       2         2         2          2          2        2         2         2
   2          2          2        2          2          2        2          2
   2       2         2          2       2         2           2)

for t_num in 0 1 2 3 4 5 6 7 8 9 10 11 12 13 14 15 16 17 18 19 20 21 22 23
24 25 26 27 28 29 30 31 32 33 34 35 36
do
{
        FIN=${TEST_RATE[t_num]}
        INTER=${DT[t_num]}
        #NUM_CYC=1
           #${CYCLES[t_num]}
        tmpt=( `echo " " | ~/scripts/freq_to_ttc.awk freq=$FIN` )
        TRAN=${tmpt[0]}
        TOTAL=${tmpt[1]}
        NUM_CYC=${tmpt[2]}
        echo $t_num $FIN $TRAN $TOTAL $NUM_CYC
        echo $t_num "   " $FIN "  " $TRAN "  " $TOTAL "  " $NUM_CYC >> ~/te
st_out/test.log
```

```
        cd ~/XPP/feedback_models/CURRENT_FORMS
 #inhibition-included tests:
        sed -e{s/_FREQ_IN_/${FIN}/,s/_AC_COND_/${AC_COND}/,s/_DC_COND_/${DC
_COND}/,s/_ALPHA_AM_/${ALPHA_AM}/,s/_ALPHA_GA_/${ALPHA_GA}/} FR_alpha_final
.form > FR_TEST.tmp.ode
        sed -e{s/_TOTAL_/${TOTAL}/,s/_TRANSIENT_/${TRAN}/,s/_DT_/${INTER}/,
s/_G_AMPA_/${G_AMPA}/,s/_G_GABA_/${G_GABA}/} FR_TEST.tmp.ode > FR_TEST2.tmp
.ode
        xpp FR_TEST2.tmp.ode -silent
        mv output.dat ~/test_out/raw_FR_data/out_freq_${FIN}_amp_${AC_COND}
_${DC_COND}.dat
 #NO inhibition tests:
        sed -e{s/_FREQ_IN_/${FIN}/,s/_AC_COND_/${AC_COND}/,s/_DC_COND_/${DC
_COND}/,s/_ALPHA_AM_/${ALPHA_AM}/,s/_ALPHA_GA_/${ALPHA_GA}/} FR_alpha_no_in
hib_final.form > FR_TEST.tmp.ode
        sed -e{s/_TOTAL_/${TOTAL}/,s/_TRANSIENT_/${TRAN}/,s/_DT_/${INTER}/,
s/_G_AMPA_/${G_AMPA}/} FR_TEST.tmp.ode > FR_TEST2.tmp.ode
        xpp FR_TEST2.tmp.ode -silent
        mv output.dat ~/test_out/raw_FR_data/out_no_inhib_freq_${FIN}_amp_$
{AC_COND}_${DC_COND}.dat
 #Move and organize files
       cd ~/test_out/raw_FR_data/
        mkdir inhib_freq_${FIN}_amp_${AC_COND}_${DC_COND}
        mkdir no_inhib_freq_${FIN}_amp_${AC_COND}_${DC_COND}
 # awk the original files to make files with columns of time and TCF, REF,
and RIN
awk '{ print $1, $6}' out_freq_${FIN}_amp_${AC_COND}_${DC_COND}.dat>inhib_
```

```
freq_${FIN}_amp_${AC_COND}_${DC_COND}/tc_freq${FIN}.awked.dat
        awk '{ print $1, $7}' out_freq_${FIN}_amp_${AC_COND}_${DC_COND}.dat
>inhib_freq_${FIN}_amp_${AC_COND}_${DC_COND}/re_freq${FIN}.awked.dat
        awk '{ print $1, $8}' out_freq_${FIN}_amp_${AC_COND}_${DC_COND}.dat
>inhib_freq_${FIN}_amp_${AC_COND}_${DC_COND}/ret_in${FIN}.awked.dat
        awk '{ print $1, $6}' out_no_inhib_freq_${FIN}_amp_${AC_COND}_${DC_
COND}.dat>no_inhib_freq_${FIN}_amp_${AC_COND}_${DC_COND}/tc_freq${FIN}.awke
d.dat
        awk '{ print $1, $7}' out_no_inhib_freq_${FIN}_amp_${AC_COND}_${DC_
COND}.dat>no_inhib_freq_${FIN}_amp_${AC_COND}_${DC_COND}/re_freq${FIN}.awke
d.dat
        awk '{ print $1, $8}' out_no_inhib_freq_${FIN}_amp_${AC_COND}_${DC_
COND}.dat>no_inhib_freq_${FIN}_amp_${AC_COND}_${DC_COND}/ret_in${FIN}.awked
.dat
##########################################################################
############################  FOURIER SCRIPT BELOW  ######################
##########################################################################
## Now run the data through a fourier awk script and append each output to
a file for
##      neuron type
~/scripts/aver_t.awk freq=${FIN} cycles=${NUM_CYC} ~/test_out/raw_FR_data/i
nhib_freq_${FIN}_amp_${AC_COND}_${DC_COND}/ret_in${FIN}.awked.dat > ~/test_
out/aved/aved_ret_amp_${FIN}.dat
~/scripts/aver_t.awk freq=${FIN} cycles=${NUM_CYC} ~/test_out/raw_FR_data/i
nhib_freq_${FIN}_amp_${AC_COND}_${DC_COND}/tc_freq${FIN}.awked.dat > ~/test
_out/aved/aved_tc_amp_${FIN}.dat
~/scripts/aver_t.awk freq=${FIN} cycles=${NUM_CYC} ~/test_out/raw_FR_data/i
```

```
nhib_freq_${FIN}_amp_${AC_COND}_${DC_COND}/re_freq${FIN}.awked.dat > ~/test
_out/aved/aved_re_amp_${FIN}.dat
~/scripts/aver_t.awk freq=${FIN} cycles=${NUM_CYC} ~/test_out/raw_FR_data/n
o_inhib_freq_${FIN}_amp_${AC_COND}_${DC_COND}/ret_in${FIN}.awked.dat > ~/te
st_out/aved/aved_no_inhib_ret_amp_${FIN}.dat
~/scripts/aver_t.awk freq=${FIN} cycles=${NUM_CYC} ~/test_out/raw_FR_data/n
o_inhib_freq_${FIN}_amp_${AC_COND}_${DC_COND}/tc_freq${FIN}.awked.dat > ~/t
est_out/aved/aved_no_inhib_tc_amp_${FIN}.dat
~/scripts/aver_t.awk freq=${FIN} cycles=${NUM_CYC} ~/test_out/raw_FR_data/n
o_inhib_freq_${FIN}_amp_${AC_COND}_${DC_COND}/re_freq${FIN}.awked.dat > ~/t
est_out/aved/aved_no_inhib_re_amp_${FIN}.dat
NUM_CYC=1 # since the data has already been normalized in the aved_t.awk sc
ript
~/scripts/fourier.awk freq=${FIN} cycles=${NUM_CYC} ~/test_out/aved/aved_re
t_amp_${FIN}.dat >> ~/test_out/foured/fed_ret_amp_${AC_COND}_${DC_COND}.dat

~/scripts/fourier.awk freq=${FIN} cycles=${NUM_CYC} ~/test_out/aved/aved_tc
_amp_${FIN}.dat >> ~/test_out/foured/fed_tc_amp_${AC_COND}_${DC_COND}.dat
~/scripts/fourier.awk freq=${FIN} cycles=${NUM_CYC} ~/test_out/aved/aved_re
_amp_${FIN}.dat >> ~/test_out/foured/fed_re_amp_${AC_COND}_${DC_COND}.dat
~/scripts/fourier.awk freq=${FIN} cycles=${NUM_CYC} ~/test_out/aved/aved_no
_inhib_ret_amp_${FIN}.dat >> ~/test_out/foured/fed_no_inhib_ret_amp_${AC_CO
ND}_${DC_COND}.dat
~/scripts/fourier.awk freq=${FIN} cycles=${NUM_CYC} ~/test_out/aved/aved_no
_inhib_tc_amp_${FIN}.dat >> ~/test_out/foured/fed_no_inhib_tc_amp_${AC_COND
}_${DC_COND}.dat
~/scripts/fourier.awk freq=${FIN} cycles=${NUM_CYC} ~/test_out/aved/aved_no
```

```
_inhib_re_amp_${FIN}.dat >> ~/test_out/foured/fed_no_inhib_re_amp_${AC_COND
}_${DC_COND}.dat
}
done
# REMOVE TEMP ODE FILES FROM .FORMS DIRECTORY:
rm ~/XPP/feedback_models/CURRENT_FORMS/*.ode
#rm ~/XPP/feedback_models/CURRENT_FORMS/output.dat
# split data into files containing a column of time and one value
awk '{print $1, $2}' ~/test_out/foured/fed_ret_amp_${AC_COND}_${DC_COND}.da
t > ~/test_out/foured/ret_F0vsFR_amp_${AC_COND}_${DC_COND}.dat
awk '{print $1, $3}' ~/test_out/foured/fed_ret_amp_${AC_COND}_${DC_COND}.da
t > ~/test_out/foured/ret_F1vsFR_amp_${AC_COND}_${DC_COND}.dat
awk '{print $1, $4}' ~/test_out/foured/fed_ret_amp_${AC_COND}_${DC_COND}.da
t > ~/test_out/foured/ret_P1vsFR_amp_${AC_COND}_${DC_COND}.dat
awk '{print $1, $5}' ~/test_out/foured/fed_ret_amp_${AC_COND}_${DC_COND}.da
t > ~/test_out/foured/ret_gammavsFR_amp_${AC_COND}_${DC_COND}.dat
awk '{print $1, $2}' ~/test_out/foured/fed_no_inhib_ret_amp_${AC_COND}_${DC
_COND}.dat > ~/test_out/foured/ret_no_inhib_F0vsFR_amp_${AC_COND}_${DC_COND
}.dat
awk '{print $1, $3}' ~/test_out/foured/fed_no_inhib_ret_amp_${AC_COND}_${DC
_COND}.dat > ~/test_out/foured/ret_no_inhib_F1vsFR_amp_${AC_COND}_${DC_COND
}.dat
awk '{print $1, $4}' ~/test_out/foured/fed_no_inhib_ret_amp_${AC_COND}_${DC
_COND}.dat > ~/test_out/foured/ret_no_inhib_P1vsFR_amp_${AC_COND}_${DC_COND
}.dat
awk '{print $1, $5}' ~/test_out/foured/fed_no_inhib_ret_amp_${AC_COND}_${DC
_COND}.dat > ~/test_out/foured/ret_no_inhib_gammavsFR_amp_${AC_COND}_${DC_C
```

```
OND}.dat
awk '{print $1, $2}' ~/test_out/foured/fed_tc_amp_${AC_COND}_${DC_COND}.dat
 > ~/test_out/foured/tc_F0vsFR_amp_${AC_COND}_${DC_COND}.dat
awk '{print $1, $3}' ~/test_out/foured/fed_tc_amp_${AC_COND}_${DC_COND}.dat
 > ~/test_out/foured/tc_F1vsFR_amp_${AC_COND}_${DC_COND}.dat
awk '{print $1, $4}' ~/test_out/foured/fed_tc_amp_${AC_COND}_${DC_COND}.dat
 > ~/test_out/foured/tc_P1vsFR_amp_${AC_COND}_${DC_COND}.dat
awk '{print $1, $5}' ~/test_out/foured/fed_tc_amp_${AC_COND}_${DC_COND}.dat
 > ~/test_out/foured/tc_gammavsFR_amp_${AC_COND}_${DC_COND}.dat
awk '{print $1, $2}' ~/test_out/foured/fed_no_inhib_tc_amp_${AC_COND}_${DC_
COND}.dat > ~/test_out/foured/tc_no_inhib_F0vsFR_amp_${AC_COND}_${DC_COND}.
dat
awk '{print $1, $3}' ~/test_out/foured/fed_no_inhib_tc_amp_${AC_COND}_${DC_
COND}.dat > ~/test_out/foured/tc_no_inhib_F1vsFR_amp_${AC_COND}_${DC_COND}.
dat
awk '{print $1, $4}' ~/test_out/foured/fed_no_inhib_tc_amp_${AC_COND}_${DC_
COND}.dat > ~/test_out/foured/tc_no_inhib_P1vsFR_amp_${AC_COND}_${DC_COND}.
dat
awk '{print $1, $5}' ~/test_out/foured/fed_no_inhib_tc_amp_${AC_COND}_${DC_
COND}.dat > ~/test_out/foured/tc_no_inhib_gammavsFR_amp_${AC_COND}_${DC_CON
D}.dat
awk '{print $1, $2}' ~/test_out/foured/fed_re_amp_${AC_COND}_${DC_COND}.dat
 > ~/test_out/foured/re_F0vsFR_amp_${AC_COND}_${DC_COND}.dat
awk '{print $1, $3}' ~/test_out/foured/fed_re_amp_${AC_COND}_${DC_COND}.dat
 > ~/test_out/foured/re_F1vsFR_amp_${AC_COND}_${DC_COND}.dat
awk '{print $1, $4}' ~/test_out/foured/fed_re_amp_${AC_COND}_${DC_COND}.dat
 > ~/test_out/foured/re_P1vsFR_amp_${AC_COND}_${DC_COND}.dat
```

```
awk '{print $1, $5}' ~/test_out/foured/fed_re_amp_${AC_COND}_${DC_COND}.dat
 > ~/test_out/foured/re_gammavsFR_amp_${AC_COND}_${DC_COND}.dat
awk '{print $1, $2}' ~/test_out/foured/fed_no_inhib_re_amp_${AC_COND}_${DC_
COND}.dat > ~/test_out/foured/re_no_inhib_F0vsFR_amp_${AC_COND}_${DC_COND}.
dat
awk '{print $1, $3}' ~/test_out/foured/fed_no_inhib_re_amp_${AC_COND}_${DC_
COND}.dat > ~/test_out/foured/re_no_inhib_F1vsFR_amp_${AC_COND}_${DC_COND}.
dat
awk '{print $1, $4}' ~/test_out/foured/fed_no_inhib_re_amp_${AC_COND}_${DC_
COND}.dat > ~/test_out/foured/re_no_inhib_P1vsFR_amp_${AC_COND}_${DC_COND}.
dat
awk '{print $1, $5}' ~/test_out/foured/fed_no_inhib_re_amp_${AC_COND}_${DC_
COND}.dat > ~/test_out/foured/re_no_inhib_gammavsFR_amp_${AC_COND}_${DC_CON
D}.dat

##    Create xmgrace graphs:
cd ~/test_out/foured/
xmgrace -param ~/xmgr/four_both.par \
-graph 0 tc_no_inhib_F0vsFR_amp_${AC_COND}_${DC_COND}.dat tc_F0vsFR_amp_${A
C_COND}_${DC_COND}.dat \
-graph 1 re_no_inhib_F0vsFR_amp_${AC_COND}_${DC_COND}.dat re_F0vsFR_amp_${A
C_COND}_${DC_COND}.dat \
-graph 2 tc_no_inhib_F1vsFR_amp_${AC_COND}_${DC_COND}.dat tc_F1vsFR_amp_${A
C_COND}_${DC_COND}.dat \
-graph 3 re_no_inhib_F1vsFR_amp_${AC_COND}_${DC_COND}.dat re_F1vsFR_amp_${A
C_COND}_${DC_COND}.dat \
-graph 4 tc_no_inhib_P1vsFR_amp_${AC_COND}_${DC_COND}.dat tc_P1vsFR_amp_${A
```

```
C_COND}_${DC_COND}.dat \
-graph 5 re_no_inhib_P1vsFR_amp_${AC_COND}_${DC_COND}.dat re_P1vsFR_amp_${A
C_COND}_${DC_COND}.dat \
-graph 6 tc_no_inhib_gammavsFR_amp_${AC_COND}_${DC_COND}.dat tc_gammavsFR_a
mp_${AC_COND}_${DC_COND}.dat \
-graph 7 re_no_inhib_gammavsFR_amp_${AC_COND}_${DC_COND}.dat re_gammavsFR_a
mp_${AC_COND}_${DC_COND}.dat &

xmgrace -param ~/xmgr/tc_2.par \
-graph 0 tc_no_inhib_F1vsFR_amp_${AC_COND}_${DC_COND}.dat tc_F1vsFR_amp_${A
C_COND}_${DC_COND}.dat \
-graph 1 tc_no_inhib_P1vsFR_amp_${AC_COND}_${DC_COND}.dat tc_P1vsFR_amp_${A
C_COND}_${DC_COND}.dat &
```

Code of 'freq_to_ttc.awk'

```
#! /bin/gawk -f
# Awk script for calculating trans, total and cycles from freq.
# freq is needed on command line
#
# script modified from on of dr. smith's ttc scripts.

BEGIN {
if (freq<=.1) {TRANSPERIODMIN = 2;}
else {TRANSPERIODMIN = 3;}
TRANSTIMEMIN = 10000;
if (freq<=.5) {RUNPERIODMIN = 1;}
else {RUNPERIODMIN = 4;}
if ((freq>10.0)||(freq<.5)) {RUNTIMEMIN = 4000;}
else {RUNTIMEMIN = 8000;}
}
END {
   period = 1.0/freq*1000; # period in ms
   trans=TRANSPERIODMIN*period;
   while (trans < TRANSTIMEMIN) {
      trans += period;
   }
   cycles=RUNPERIODMIN;
   run=cycles*period;
   while (run < RUNTIMEMIN) {
      cycles += 1;
      run=cycles*period;
```

```
    }
    total = trans+run;
    print trans, total, cycles;
}
```

Code of 'aver_t.awk'

```
#! /bin/gawk -f
# Awk script
#   This script sums all cycles of a certain run into the a histogram
#  one period in length.
# freq is needed on command line
# cycles is needed on command line
BEGIN {
   i=0;
   j=0;
}
{
   # read in periodic histogram
   htemp[i]=$2;
   ttemp[i++]=$1;
}
END {
   BINNUM=128;
   start_t=ttemp[0];
   period = 1.0/freq*1000;
   bin_lngth=period/BINNUM;
   k=0; #counter to run over all cycles
   for (i=1; i<=BINNUM; i++ )   {h[i]=0; norm_val[i]=0;}
   # Time-based averaging:
   for (j=0; j<cycles; j++)
for (j2=1; j2<=BINNUM; j2++) {
t[j2]=j2*bin_lngth;
```

```
while ((ttemp[k]<=j2*bin_lngth+j*period+start_t)&&(ttemp[k]!="")) {
h[j2]=h[j2]+htemp[k];
k++;
norm_val[j2]++;
}
}
   for (i=1; i<=BINNUM; i++ ) h[i]=h[i]/norm_val[i];
   for (i=1; i<=BINNUM; i++ ) {
      print t[i],h[i];
      }
}
```

Code of 'fourier.awk':

```
#! /bin/gawk -f
# Awk script for calculating response measures from periodic histogram
# freq is needed on command line
# cycles is needed on command line

BEGIN {
   i=0;
}
{
   period = 1.0/freq;

   # read in periodic histogram
   h[i++]=$2;
   BINNUM=i; # total number of bins, 128
}
END {
   TWOPI = 2.0*3.1415927;
   # N is total power
   N=0;
   for (i=0; i<BINNUM; i++) N += h[i]^2;
   # a0 is just rate; p0=0 (no phase for rate)
   # a1 is stimulus driven response; p1 is phase of this response
   for (m=0; m<=1; m++) { # loop through modes 0 and 1
      a[m] = 0; b[m] = 0;
      for (i=0; i<BINNUM; i++) {
         a[m] += h[i]*cos(TWOPI*m*i/BINNUM);
```

```
      b[m] += h[i]*sin(TWOPI*m*i/BINNUM);
      }
   r[m] = sqrt(a[m]^2+b[m]^2);
   p[m] = -atan2(b[m],a[m])/TWOPI;
}
N  = N/cycles^2;
A0 = r[0]/cycles;
A1 = r[1]/cycles;
P1 = p[1];
# OLD IN : if ( N!=0 ) IN = (N-(A0^2+2*A1^2)/BINNUM)/N ;
if ( N-A0^2/BINNUM !=0 ) IN = (N-(A0^2+2*A1^2)/BINNUM)/(N-A0^2/BINNUM);
else IN = 0;
# Output in the following order:
#  Col         Meaning
#  $1     A0 (DC spikes/sec)
#  $2     A0 (DC spikes/cycle)
#  $3     F1=2*A1 (AC spikes/sec)
#  $4     F1=2*A1 (AC spikes/cycle)
#  $5     -0.5 < p[1] < 0.5
#  $6     0 < IN < 1
# print freq*A0/BINNUM, A0/BINNUM, 2*freq*A1/BINNUM, 2*A1/BINNUM, P1, IN;
# Mult the F0 and F1 by 1000 to convert from millisec to sec to be more easil
y comparable to the FR
print freq, A0/BINNUM*1000, 2*A1/BINNUM*1000, P1, IN;
}
```

Code of 'FR_alpha_final.form':

```
#
# TC-RE FR model sln with alpha-fn in s-vars
#       (feedback GABA-inhibition (biological model))
#
#  This is the .form file to use for param studies
#    of the model's behavoir
#

# parameters to change trial by trial (FR=firing rate)
par Fin=_FREQ_IN_ AC_cond=_AC_COND_ DC_cond=_DC_COND_
par gampa=_G_AMPA_ ggaba=_G_GABA_ alphaampa=_ALPHA_AM_ alphagaba=_ALPHA_GA_
@ total=_TOTAL_,dt=_DT_,trans=_TRANSIENT_,maxstor=1000000,bounds=500
dsgabax/dt=alphagaba*(fre(veffr(geffr(sampay)),taur(geffr(sampay)))-sgabax)
dsgabay/dt=alphagaba*(sgabax-sgabay)
dsampax/dt=alphaampa*(ftc(vefft(gefft(sgabay,gret(t)),gret(t)),taut(gefft(sgabay
,gret(t))))-sampax)
dsampay/dt=alphaampa*(sampax-sampay)

ftc(vefft,taut)=if((vefft>vthetat)&(((taut*ln((vefft-vresett)/(vefft-vthetat)))^
(-1))>0))then((taut*ln((vefft-vresett)/(vefft-vthetat)))^(-1))else(0)
fre(veffr,taur)=if((veffr>vthetar)&((taur*ln((veffr-vresetr)/(veffr-vthetar)))^(
-1)))then((taur*ln((veffr-vresetr)/(veffr-vthetar)))^(-1))else(0)
vefft(gefft,gret)=(glt*vlt+gret*vret+ggaba*sgabay*vgaba)/gefft
veffr(geffr)=(glr*vlr+gampa*sampay*vampa)/geffr
gefft(sgabay,gret)=(glt+gret+ggaba*sgabay)
geffr(sampay)=(glr+gampa*sampay)
```

```
taut(gefft)=c/gefft
taur(geffr)=c/geffr

#ret input for linear tests:
#gret(t)=DC_cond*t
#ret input for drifting grating type tests
#    (eq in the form DC_cond+AC_cond*cos(2*pi*FR*t))
gret(t)=if((DC_cond+AC_cond*(cos(2*pi*Fin/1000*t)))>0)then(DC_cond+AC_cond*(cos(
2*pi*Fin/1000*t)))else(0)
aux TCf=ftc(vefft(gefft(sgabay,gret(t)),gret(t)),taut(gefft(sgabay, gret(t))))
aux REf=fre(veffr(geffr(sampay)),taur(geffr(sampay)))
aux RIn=gret(t)
init   sgabax=.0   sampax=.0  sgabay=.0   sampay=.0
par c=1  glt=0.03  glr=0.03
par vlt=-65 vthetat=-35 vresett=-50 vgaba=-85
par vlr=-65 vthetar=-35 vresetr=-50 vampa=0
par vret=0
done
```

Code of 'FR_alpha_no_inhib_final.form':

```
#
# TC-RE FR model sln with alpha-fn in s-vars
#     Inhibitionless model (since ggaba=0)
#       (feedback GABA-inhibition (biological model))
# This is the .form file to use in parameter studies of the
#    model's behavior
#


# parameters to change trial by trial
par Fin=_FREQ_IN_ AC_cond=_AC_COND_ DC_cond=_DC_COND_
par gampa=_G_AMPA_ alphaampa=_ALPHA_AM_ alphagaba=_ALPHA_GA_
par ggaba=0
@ total=_TOTAL_,dt=_DT_,trans=_TRANSIENT_,maxstor=1000000,bounds=500
#i thought i had removed the inhibition before, but couldn't figure out how i ha
d done it, so i
#   changed these sgaba vars so they would always be zero, to make sure inhibiti
on plays no role
dsgabax/dt=0
#was:  dsgabax/dt=alphagaba*(fre(veffr(geffr(sampay)),taur(geffr(sampay)))-sgaba
x)
dsgabay/dt=0
#was:  dsgabay/dt=alphagaba*(sgabax-sgabay)
dsampax/dt=alphaampa*(ftc(vefft(gefft(sgabay,gret(t)),gret(t)),taut(gefft(sgabay
,gret(t))))-sampax)
dsampay/dt=alphaampa*(sampax-sampay)
```

```
ftc(vefft,taut)=if((vefft>vthetat)&(((taut*ln((vefft-vresett)/(vefft-vthetat)))^
(-1))>0))then((taut*ln((vefft-vresett)/(vefft-vthetat)))^(-1))else(0)
fre(veffr,taur)=if((veffr>vthetar)&((taur*ln((veffr-vresetr)/(veffr-vthetar)))^(
-1)))then((taur*ln((veffr-vresetr)/(veffr-vthetar)))^(-1))else(0)
vefft(gefft,gret)=(glt*vlt+gret*vret+ggaba*sgabay*vgaba)/gefft
veffr(geffr)=(glr*vlr+gampa*sampay*vampa)/geffr
gefft(sgabay,gret)=(glt+gret+ggaba*sgabay)
geffr(sampay)=(glr+gampa*sampay)
taut(gefft)=c/gefft
taur(geffr)=c/geffr
#ret input for linear tests:
#gret(t)=DC_cond*t
#ret input for drifting grating type tests
gret(t)=if((DC_cond+AC_cond*(cos(2*pi*Fin/1000*t)))>0)then(DC_cond+AC_cond*(cos(
2*pi*Fin/1000*t)))else(0)
aux TCf=ftc(vefft(gefft(sgabay,gret(t)),gret(t)),taut(gefft(sgabay, gret(t))))
aux REf=fre(veffr(geffr(sampay)),taur(geffr(sampay)))
aux RIn=gret(t)
init   sgabax=.0   sampax=.0  sgabay=.0   sampay=.0
par c=1  glt=0.03  glr=0.03
par vlt=-65 vthetat=-35 vresett=-50 vgaba=-85
par vlr=-65 vthetar=-35 vresetr=-50 vampa=0
par vret=0
done
```

Code of 'total_lin.m':

```
% this file derives all necessary equations for the linear analysis
%     and performs linear analysis and plots results (12-2-02)
% plotting parameters:
BOTTOM = -3
TOP = 3
NUM = 200
AXLO = 10^(BOTTOM+1); AXHI = 10^(TOP-1)
syms sAx sAy sGx sGy Gret Gret0 Gret1 omega
Gtcl = 0.03
Vtcl = -65
Vtcreset = -50
Vtctheta = -35
Grel = 0.03
Vrel = -65
Vrereset = -50
Vretheta = -35
VG = -85
VA = 0
Vret = 0
gbarGA = .85  %constant for now
gbarAM = .1
alphaG = 0.1
alphaA = 0.1
C = 1
% Set set-point vars % check these values before final:
sAx_set =  0.0595
```

```
sAy_set =  0.0595

sGx_set =  0.0925

sGy_set =  0.0925

Gret_set = 0.05

% Set input vars

Gret0__ = Gret_set

Gret1__ = 0.005

fret = logspace(BOTTOM, TOP, NUM)

omega__ = fret*2*pi/1000

% State f-vars

tautc = C/(Gtcl + Gret + gbarGA*sGy)

Vtceff = (Gtcl*Vtcl + Gret*Vret + gbarGA*sGy*VG)/ (Gtcl + Gret + gbarGA*sGy)

taure = C/(Grel + gbarAM*sAy)

Vreeff = (Grel*Vrel + gbarAM*sAy*VA)/ (Grel + gbarAM*sAy)

ftc = (tautc*log((Vtceff - Vtcreset)/(Vtceff - Vtctheta)))^(-1)

fre = (taure*log((Vreeff - Vrereset)/(Vreeff - Vretheta)))^(-1)

% Determine k-vars

kTC0 = subs(ftc, [Gret, sGy], [Gret_set, sGy_set])

kTCE = subs(diff(ftc, Gret), [Gret, sGy], [Gret_set, sGy_set])

kTCI = subs(diff(ftc, sGy), [Gret, sGy], [Gret_set, sGy_set])

kRE0 = subs(fre, sAy, sAy_set)

kREE = subs(diff(fre,sAy), sAy, sAy_set)

% Determine s0 and s1 vars

    % non-time-varying terms:

    [ sAx0, sAy0, sGx0, sGy0 ] = solve ( ...

        '-alphaA*sAx0 +alphaA*kTCI*sGy0 +alphaA*(kTC0+kTCE*Gret0) = 0', ...

        'alphaA*sAx0 -alphaA*sAy0 = 0', ...
```

```
        'alphaG*kREE*sAy0 -alphaG*sGx0 +alphaG*kRE0 = 0', ...
        'alphaG*sGx0 -alphaG*sGy0 = 0' )
    % time-varying terms (those *e^(i*omega*t)):
    [ sAx1, sAy1, sGx1, sGy1 ] = solve ( ...
        '-alphaA*sAx1 + alphaA*kTCI*sGy1 +alphaA*(kTCE*Gret1) = (-1)^(1/2)*
omega*sAx1 ', ...
        'alphaA*sAx1-alphaA*sAy1 = (-1)^(1/2)*omega*sAy1', ...
        'alphaG*kREE*sAy1-alphaG*sGx1 = (-1)^(1/2)*omega*sGx1', ...
        'alphaG*sGx1-alphaG*sGy1 = (-1)^(1/2)*omega*sGy1' )
% reassign s0 and s1 vars to be numeric
sAx0_ = subs(subs(sAx0), Gret0, Gret0__)
sAy0_ = subs(subs(sAy0), Gret0, Gret0__)
sGx0_ = subs(subs(sGx0), Gret0, Gret0__)
sGy0_ = subs(subs(sGy0), Gret0, Gret0__)
sAx1_ = subs(subs(subs(sAx1), Gret1, Gret1__), omega, omega__)
sAy1_ = subs(subs(subs(sAy1), Gret1, Gret1__), omega, omega__)
sGx1_ = subs(subs(subs(sGx1), Gret1, Gret1__), omega, omega__)
sGy1_ = subs(subs(subs(sGy1), Gret1, Gret1__), omega, omega__)
% Determine f0 and f1 vars
ftc0 = kTC0 + kTCI*sGy0_ + kTCE*Gret0__
ftc1 = kTCI*sGy1_ + kTCE*Gret1__
fre0 = kRE0 + kREE*sAy0_
fre1 = kREE*sAy1_
% so finally, the DC, AC, and phase of the output:
DC_amp = abs(ftc0)
AC_amp = abs(ftc1)
phase = angle(ftc1)
```

```
%keep phase from switching to negative (necessary if phase is > 1/2 of a cy
cle):
%for i = 1:NUM
% if phase(i) < -.05
% phase(i) = phase(i) + 2*pi
% end
%end
%change phase from radians to cycles:
phase = phase/(2*pi)
% plots:
AC_plot = subplot(2,1,1)
semilogx(fret,AC_amp*1000,'LineWidth',2)
axis([AXLO AXHI 0 120])
text(10^(-1),128,'TC Response (F_1, P_1)','Fontsize',14)
%set(AC_plot,'XTick',[1e-05 1e-03 1e-01 10 100])
%xlabel('','FontSize',12,'VerticalAlignment','bottom')
ylabel('F_1, Modulating TC Firing Rate (Hz)','FontSize',12,'HorizontalAlign
ment','left')
phase_plot = subplot(2,1,2)
semilogx(fret,phase,'LineWidth',2)
axis([AXLO AXHI -.23 .22])
%text(10^(-1),0.125,'Phase vs Input Frequency','Fontsize',14)
xlabel('F_{ret} (Hz)','FontSize',12,'VerticalAlignment','bottom')
ylabel('P_1, Phase Change (cycles)','FontSize',12,'HorizontalAlignment','le
ft')
return
```

References

[1] P. Dayan and L.F. Abbott. *Theoretical Neuroscience: Computational and Mathematical Modeling of Neural Systems.* MIT Press, Cambridge, MA, 2001.

[2] Bard Ermentrout. *Software, Environments, and Tools 14: Simulating, Analyzing, and Animating Dynamical Systems: A Guide to XPPAUT for Researchers and Students.* SIAM, 2002.

[3] Walter J. Hendelman. *Student's Atlas of Neuroanatomy.* W. B. Saunders, Philadelphia, PA, 1994.

[4] Hille. *Ion Channels of Excitable Membranes.* Sinauer As. Inc., Sunderland, Massachusetts, 2001.

[5] R.M. Shapley and P. Lennie. Spatial frequency analysis in the visual system. *Ann. Rev. Neurosci.*, 8:547–583, 1985.

[6] G.D. Smith, C.L. Cox, S.M. Sherman, and J. Rinzel. Fourier analysis of sinusoidally-driven thalamocortical relay neurons and a minimal intergrate-and-fire-or-burst model. *J. Neurophysiol.*, 83(1):588, 2000.

[7] G.D. Smith, C.L. Cox, S.M. Sherman, and J. Rinzel. A firing-rate model of spike-frequency adaptation in sinusoidally-driven thalamocortical relay neurons. *Thalamus and Related Systems*, 11:1–22, 2001.

[8] Gregory D. Smith. The effect of feedback inhibition on sensory relay by the thalamus. 2001.

[9] Gregory D. Smith. Personal communication, 2002–2003.